SE-128T
CONTRACT NAS 9-12105
DRL LINE ITEM 5

NASA CR-
147545

Beech Aircraft Corporation

Boulder, Colorado

CODE IDENT. NO. 07399

THERMAL DESIGN REPORT

HYDROGEN THERMAL TEST ARTICLE (HTTA)

Engineering Report ER 15464

Issue Date: November 19, 1971

APPROVED BY J. E. Bell
J. E. Bell
Manager of Engineering

TABLE OF CONTENTS

TABLE OF CONTENTS (contd)

PREFACE

This report was prepared by Beech Aircraft Corporation, Boulder Division, Boulder, Colorado, under Contract NAS9-12105, Hydrogen Thermal Test Article (HTTA), from the Manned Spacecraft Center, Houston, Texas.

The tasks which were accomplished during the analytic study portion of this program are: (1) selection of thermally optimized insulation systems for a double-walled liquid hydrogen storage vessel both for the requirements of the Space Shuttle Orbital Maneuvering System (7-day mission) and of an extended mission (180-days); and (2) development of an analytic technique to be used for predicting performance characteristics of the insulation configuration selected for fabrication. The installed insulation system will be selected on the basis of 180-day mission requirements. The approaches used in performing this study and the recommended insulation systems for the two missions are described in this report. Thermal performance estimates for the recommended configurations are presented.

NOMENCLATURE

SYMBOLS:

A	Area (ft^2)
C_P	Specific heat (Btu/lb-^oR)
H	Enthalpy (Btu/lb)
k	Thermal conductivity (Btu/ft-hr-^oR)
K	Conductance (Btu/^oR), $Q = K\triangle T$
L	Conduction length (ft)
$\dot{m}$	Boiloff rate (lb/hr)
N	Number of multilayer insulation layers
$\tilde{N}$	Number of multilayer insulation layers per inch
q	Heat flux (Btu/ft^2-hr)
Q	Heat transfer rate (Btu/hr)
T	Temperature (^oR)
ϵ_{eff}	Effective multilayer blanket emittance, $q = \sigma \epsilon_{eff} (T_H^4 - T_C^4)$
ϵ_T	Total effective multilayer emittance from outer shell to pressure vessel
ϵ_{TRA}	Surface emittance of aluminized mylar at 540^oR
ϵ_{TRG}	Surface emittance of goldized mylar at 540^oR
ϵ_{TRS}	Surface emittance of silverized mylar at 540^oR
ϵ_1	Effective multilayer blanket emittance between outer shell and vapor-cooled shield
ϵ_2	Effective multilayer blanket emittance between vapor-cooled shield and pressure vessel

SYMBOL

θ	Heat input required to expel a unit mass of fluid from the pressure vessel (Btu/lb)
σ	Stephan-Boltzmann constant, 1.714×10^{-9} (Btu/ft^2-hr-$^\circ$R^4)

SUBSCRIPTS

BS	Boiler shield
C	Cold boundary
H	Hot boundary
L	Liquid vented from pressure vessel
OS	Outer shell
PV	Pressure vessel
R	Radiation
V	Vapor or vapor vented from pressure vessel
VCS	Vapor-cooled shield
1	Between outer shell and vapor-cooled shield
2	Between vapor-cooled shield and pressure vessel

ABBREVIATIONS

DAM	Double-aluminized mylar
DSM	Double-silverized mylar
MLI	Multilayer insulation
PV	Pressure vessel
VCS	Vapor-cooled shield

1.0 INTRODUCTION

The goals of this study program are: (1) selection of thermally optimized insulation systems for a double-walled hydrogen storage vessel commensurate with the requirements of the Space Shuttle Orbital Maneuvering System (7-day mission) and of an extended (180-day) mission, (2) development of an analytic technique to aid in evaluating candidate insulation systems and to predict performance characteristics for the selected configurations, and (3) enumeration of areas which merit further investigation.

The term "insulation system" as used here includes insulation materials (e.g., passive radiation barriers and spacers), active insulation components (e.g., vapor-cooling system), phase-separating devices (e.g., devices such as a retention screen internal to the pressure vessel which will prevent liquid being vented from the pressure vessel during constant-pressure, zero-g storage), and structural support elements which contribute to the heat leak.

A thermally optimized system is one which provides storage and delivery capability with minimum weight penalty, cost and maintenance, and with maximum reliability, safety, durability, and predictability. All elements of the insulation system, except phase separating devices, must be vacuum compatible. Phase separating devices need not be vacuum compatible because they are contained inside the pressure vessel.

In determining the weight penalty for a given configuration, both the total fluid boiloff and the insulation system weights must be considered. For this study, it is assumed that fluid boiloff is vented overboard and not used for cooling any other equipment. A configuration which is weight optimized for 7-day constant pressure storage will very likely not be weight optimized for 180-day storage.

The program goals were accomplished through the following steps:

(1) definition of thermal performance and operational requirements for the two missions,

(2) selection of several insulation system configurations which best meet the thermal performance and operation requirements,

(3) definition of design selection criteria to use in selecting the best-suited insulation materials,

(4) selection of insulation materials commensurate with these criteria,

(5) flat plate performance testing of selected multilayer insulation materials,

(6) performance of thermal analyses required to determine which configurations provide least weight penalty for each of the two missions,

(7) development of an analytic technique to make accurate thermal performance predictions for the selected configurations during all modes of operation, with flat plate multilayer insulation performance test results and oxygen thermal test article, OTTA (Reference 1) performance test results used to improve estimates of multilayer insulation performance for these final performance predictions, and

(8) analytic estimates of the effects of storage pressure and ullage size upon thermal performance characteristics.

This report describes the approaches used to accomplish the individual tasks listed above. Results of these study tasks, recommended insulation systems for both the 7-day mission and 180-day mission, and predicted performance characteristics for the recommended systems are contained in this report.

Areas which merit additional investigation and analysis are discussed.

2.0 SELECTION OF INSULATION SYSTEM MATERIALS AND CANDIDATE CONFIGURATIONS

2.1 Literature Surveys

Surveys of the literature were performed in three areas as described in this section.

2.1.1 Multilayer Insulation Studies

Beech's knowledge of multilayer insulation systems is the result of experience over a period of 10 years in designing and applying such systems to cryogenic tankage. During this time, Beech has kept abreast of improvements and new developments in multilayer insulation systems which were presented in the literature.

Most current efforts concerning multilayer insulation are directed toward improving estimates of multilayer insulation performance as

installed on tankage. Reference 2 reports the most recent and most applicable study of this type. Four multilayer insulation systems were investigated in this study:

(1) double-aluminized 1/4-mil mylar with double silk net spacers;

(2) double-goldized 1/4-mil mylar with double silk net spacers;

(3) crinkled, single-aluminized 1/4-mil mylar; and

(4) double-aluminized mylar with tissuglas spacers.

Based on experimental data reported in Reference 2, correlations were constructed to compute heat flux through these four multilayer insulation systems. The system with goldized mylar was found to be significantly superior on a performance-to-weight basis.

The surface reflectance of silverized mylar is approximately 8% lower than that of goldized mylar throughout the temperature range of interest. It is consequently assumed that the reported performance correlation for goldized mylar can also be used for silverized mylar with the application of an 8% reduction factor.

The only new development in multilayer insulation materials is the continued improvement of Superfloc as reported in Reference 3. While Superfloc appears very attractive on a performance-to-weight basis, it is presently unavailable on a large scale production basis and requires further development in layup techniques. These conclusions are the result of recent negotiations between Beech and the Convair Division of General Dynamics, which is one of several companies developing Superfloc.

Relative advantages and disadvantages of various multilayer insulation materials are discussed in more detail in Section 2.3.

2.1.2 Shuttle Studies

A review of the Shuttle Orbiter Study reports gives an overall view of some considerations for the selection of an insulation system for the HTTA.

The hydrogen tank insulation system baseline configuration was reported in the shuttle studies, (Reference 4). A flexible purge bag and 50 layers of double-goldized multilayer insulation had been selected.

However, the recent studies dealing with a cryogenic orbital maneuvering propulsion system have indicated that purge requirements and weight were sufficiently higher than previously predicted to warrant consideration of a dewar-type storage system from a weight optimization standpoint.

In Reference 4 several thermodynamic venting configurations were considered wherein the refrigeration available in the vented fluid was utilized to intercept part of the heat leak to the storage vessel. These venting configurations consisted of an expansion valve inside the pressure vessel with either a boiler shield external to the pressure vessel or one of two types of heat exchanger inside the pressure vessel.

Other prime contractors have indicated similar baseline configurations without specifically identifying the actual insulation components.

2.1.3 Shuttle Cryogenic Supply System Optimization Study

The task reports (Reference 5) for the cryogenic optimization study contain detailed information on several multilayer insulation composites; however, this information does not provide an insight to the insulation optimization since the overall system effects are not included.

From Reference 5 the selected insulation configuration for a cryogenic orbital manuevering propulsion system hydrogen tank is two inches (approximately 40 layers) of Superfloc without vapor cooling shields. Although this is not an optimized insulation system for a single tank situation, it is a near optimum configuration for the overall system. An insulation optimization analysis with consideration of the overall system is a multiple parameter problem requiring many assumptions and consideration of factors such as requirements for cooling fluid to pumps, transfer lines, orientation devices, and other storage vessels. Selection of the hydrogen tank insulation system which is optimized with respect to overall system requirements is consequently tedious and difficult. Overall system requirements will not be considered in determining the optimum insulation system for this test article.

2.2 Design Criteria

Thermal performance and operational requirements and environmental conditions determine the optimum insulation system and materials for a cryogenic storage system. The design criteria which were used to select the optimum insulation system for the HTTA are listed in the following two sections for the 7-day and 180-day missions. As directed by contract change 1S, the 180-day mission has been selected as the basis for designing the insulation system of the test article.

2.2.1 7-Day Mission Design Criteria

Mission: 7-day storage with 30-day flight exposure, 100 missions, short ground time.

Fluid: Liquid hydrogen, it is assumed that approximately half the fluid is used immediately after orbit insertion for initial orbital maneuvers (see Figure 1).

PV Volume: 800 ft^3 (cylindrical shape).

Storage Pressure: 15 to 50 psia (constant).

LH_2 Delivery Rate: 8 lb/sec (2 to 4 psi subcooled).

Environment: Zero-g, external temperature of 600°R.

Loads (Full Tank): 3.3 g vertical, 1.0 g horizontal.

Annular Vacuum: 1×10^{-5} torr or less.

2.2.2 180-Day Mission Design Criteria

Mission: 180-day storage, one mission.

Fluid: Liquid hydrogen, maximum fluid retention for 180 days.

PV Volume: 800 ft^3 (cylindrical shape).

Storage Pressure: 15 to 50 psia (constant).

LH_2 Delivery Rate: 8 lb/sec (2 to 4 psi subcooled).

Environment: Zero-g, external temperature of 540°R.

Loads (Full Tank): 3.3 g vertical, 1.0 g horizontal.

Annular Vacuum: 1×10^{-5} torr or less.

2.3 Multilayer Insulation Selection

Because of the relatively large ratio of surface area to stored fluid weight, over 90% of the heat leak to this tank will be by radiation when a thermally optimized pressure vessel support system is employed. Based on Beech experience and information in the literature, a multilayer insulation is much more effective than any other type of insulation on a performance-to-weight basis for protection against radiation.

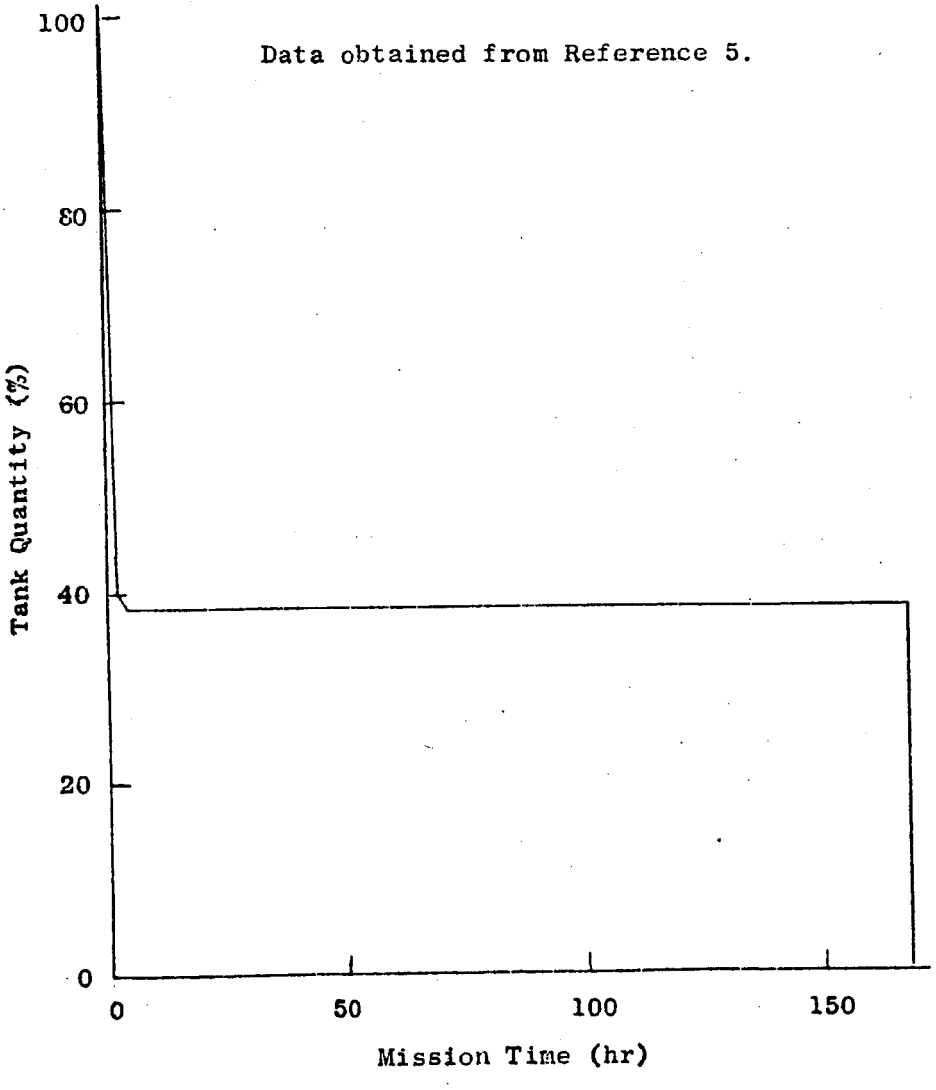

Figure 1 - Fluid Usage for Space Shuttle Orbital Maneuvering System Hydrogen Tank

Other types of insulation have consequently been eliminated from further consideration in this study.

A comparative evaluation technique (described in Reference 6) was used to select the multilayer insulation materials which are best suited for each of the two missions being considered in this study. A brief explanation of this technique follows. A more comprehensive discussion is contained in Reference 6.

Based on the design requirements given in Sections 2.2.1 and 2.2.2, design selection criteria were chosen for the purpose of evaluating candidate multilayer insulation materials. These criteria represent the factors which must be considered in selecting the most suitable insulation materials for spacecraft cryogenic tankage. These design selection criteria are listed below.

(1) Thermal Performance
(2) Weight
(3) Susceptibility to all Environments
(4) Reliability
(5) Durability and Useful Life
(6) Required Maintenance
(7) Predictability of Thermal Performance
(8) Required Development
(9) Materials Availability
(10) Cost (installed)
(11) Ground Hold Requirements

These design selection criteria are assigned weighting factors (from 1 to 10) which reflect their relative importance for a given set of mission and performance requirements. The most important criteria are given weighting factors of 10. These weighting factors were qualitatively chosen on the basis of Beech experience and information contained in the literature (Reference 6 in particular).

Candidates are evaluated by listing them in order of desirability (1 for most desirable) for each of the selection criteria. Rankings are based on knowledge acquired from Beech experience and from the literature. A total score for each candidate is obtained by summing the products of weighting factors and rank assignments. The candidate with lowest total score is judged best.

Many types of multilayer insulation materials are available and capable of providing adequate thermal protection for this tank. Eight of the most attractive multilayer insulation systems were chosen and evaluated by the method described above. Results of this evaluation are shown in Tables I and II for the 7-day mission and 180-day mission, respectively.

TABLE I

MULTILAYER INSULATION EVALUATION MATRIX FOR 7-DAY MISSION

	WEIGHTING FACTOR	ALUMINIZED MYLAR, 1 NYLON NET SPACER	GOLDIZED MYLAR, 1 NYLON NET SPACER	SILVERIZED MYLAR, 1 NYLON NET SPACER	NRC-2, NO SPACER	0.001" ALUMINUM FOIL, 1 NYLON NET SPACER	SUPERFLOC, NO SPACER	ALUMINIZED MYLAR, 2 SILK NET SPACERS	ALUMINIZED MYLAR, POLYURETHANE FOAM SPACER
SUSCEPTIBILITY TO ALL ENVIRONMENTS	10	2	3	6	4	6	5	1	7
WEIGHT	10	6	4	3	2	8	1	5	7
DURABILITY AND USEFUL LIFE	8	2	2	6	8	4	5	2	7
THERMAL PERFORMANCE	10	ALL CANDIDATES CONSIDERED CAPABLE OF REQUIRED PERFORMANCE, WITH NECESSARY NUMBER OF LAYERS							
RELIABILITY	9	ALL CANDIDATES EQUAL							
REQUIRED MAINTENANCE	8	3	3	3	6	3	7	3	8
PREDICTABILITY OF THERMAL PERFORMANCE	8	4	4	4	4	8	4	4	4
COST - INSTALLED		1	8	2	6	3	7	5	4
GROUND HOLD REQUIREMENTS	5	ALL CANDIDATES EQUAL							
REQUIRED DEVELOPMENT	8	ALL CANDIDATES DEVELOPED							
MATERIALS AVAILABILITY	8	2.5	6	5	2.5	7	8	2.5	2.5
T O T A L		177	230	244	254	331	287	177	332
P L A C E		1	3	4	5	8	6	2	7

NOTES: 1. Superfloc information is limited for outgassing, availability, and cost data.

2. Where ratings were equal, average position value was used.

TABLE II

MULTILAYER INSULATION EVALUATION MATRIX FOR 180-DAY MISSION

	WEIGHTING FACTOR	ALUMINIZED MYLAR, 1 NYLON NET SPACER	GOLDIZED MYLAR, 1 NYLON NET SPACER	SILVERIZED MYLAR, 1 NYLON NET SPACER	NRC-2, NO SPACER	0.001" ALUMINUM FOIL, 1 NYLON NET SPACER	SUPERFLOC, NO SPACER	SILVERIZED MYLAR, 2 SILK NET SPACERS	ALUMINIZED MYLAR, POLYURETHANE FOAM SPACER
SUSCEPTIBILITY TO ALL ENVIRONMENTS	8	2	1	4.5	3	6	7	4.5	8
WEIGHT	6	6	4	3	5	8	1	2	7
RELIABILITY	10	2.5	2.5	5.5	2.5	2.5	7.	5.5	8
THERMAL PERFORMANCE	10	ALL CANDIDATES CONSIDERED CAPABLE OF REQUIRED PERFORMANCE, WITH NECESSARY NUMBER OF LAYERS							
DURABILITY AND USEFUL LIFE	7	ALL CANDIDATES EQUAL							
REQUIRED MAINTENANCE	9	3	3	3	6	3	7	3	8
PREDICTABILITY OF THERMAL PERFORMANCE	10	5	2.5	2.5	7	8	5	1	5
COST - INSTALLED	6	2	8	2	6	4	7	2	5
GROUND HOLD REQUIREMENTS		ALL CANDIDATES EQUAL							
REQUIRED DEVELOPMENT		ALL CANDIDATES DEVELOPED							
MATERIALS AVAILABILITY	5	3	3	3	3	7	8	3	6
T O T A L		177	172	188	254	287	327	167	368
P L A C E		3	2	4	5	6	7	1	8

NOTES: 1. Superfloc information is limited for outgassing, availability, and cost data.

2. Where ratings were equal, average position value was used.

Multilayer insulation cost and weight ratings were based on the number of layers which were considered to provide approximately the same amount of insulation for each candidate. Listed below are some of the factors which affected the evaluations:

(1) 0.001-inch Al foil is 5 times heavier and more susceptible to tearing than 1/4-mil mylar.

(2) Net and foam spacers provide tear strength to the multilayer insulation.

(3) Vacuum-deposited coatings are susceptible to degradation due to abrasion and corrosion.

(4) Silver coatings are less durable than gold or aluminum coatings.

(5) Silver coatings provide a surface emittance slightly better than gold and almost twice as good as aluminum.

(6) An installed system of goldized mylar costs approximately 5 times more than aluminized or silverized mylar. This is based on estimated costs of materials, fabrication, and installation for the numbers of layers considered to give the same thermal performance in each case.

(7) Superfloc is presently unavailable in the required quantity and requires development in layup techniques.

(8) Polyurethane foam spacing material was rated low in useful life and maintainability because of possible outgassing and degradation after prolonged vacuum exposure.

Based on the results shown in Tables I and II, the following multilayer insulation materials are recommended:

7-Day Mission: Double-aluminized 1/4-mil mylar with double silk net spacer.

180-Day Mission: Double-silverized 1/4-mil mylar with double silk net spacer.

Flat plate insulation testing at Beech/Boulder (see Section 5.0 for description and results of this testing), currently indicates that double-silk net and single-nylon net are equally effective spacer materials at higher temperature levels where radiation is relatively large and conduction in the multilayer insulation is insignificant.

However, at lower temperature levels where conduction becomes significant, the double-silk net appears to provide superior performance. Consequently, since nylon net is cheaper than double-silk net, nylon net could be used above the vapor-cooled shield and double-silk net used below the vapor-cooled shield in order to reduce cost.

Testing is currently in progress at Beech/Boulder to verify the vacuum compatibility of both nylon and silk net. Previous experience with the Beech Insulation Comparator indicates that there is no problem for either material.

2.4 Support Structures

The insulation system contains two types of support structures: the pressure vessel support system and the structural elements required to support the vapor-cooling system.

A thermally optimized support system provides reliable support with minimum hindrance to the insulation layup and performance and is vacuum compatible. Based on these criteria, a tension band pressure vessel support system using filament-wound glass composite bands is recommended.

Bands consisting of S/HTS glass filament with Resin No. 2, NASA Contract NAS3-6287, have been used by Beech on previous cryogenic tankage and are proposed for the HTTA. Currently available information indicates that these bands are vacuum compatible when a vacuum baking process is used prior to installation. Testing is scheduled at Beech to verify this.

These bands exhibit extremely high ratios of strength-to-weight and strength-to-thermal conductivity (design stress = 200,000 psi, density = 0.075 lb/in^3, effective thermal conductivity between 40 and 600°R = 0.17 Btu/ft-hr-°R). Because of the small required cross-sectional areas of these bands, penetration sizes and associated effects are reduced. The proposed pressure vessel support system consists of 22 bands which are each approximately 2 feet long and 0.12 in^2 in cross section

The vapor-cooled shield and boiler shield will be made of thinnest practical material in order to minimize weight. These shields will be supported from the pressure vessel with stand-off pins made of low thermal conductivity material (e.g., nylon) with minimum cross-sectional area design. It is anticipated that approximately fifty, uniformly distributed supports will be required.

2.5 Candidate Vent System Configurations

Four vent configurations were chosen for evaluation in order to

determine which provides least weight penalty for each of the two missions; they are:

(1) Vapor-cooled shield only.

(2) Vapor-cooled shield with complete boiler shield.

(3) Vapor-cooled shield with boiler shield on cylindrical portion of vessel only.

(4) No vapor cooling (phase separating device required to prevent liquid being vented from the pressure vessel during zero-g operation).

In order to determine the weight penalty for each configuration, the optimum number of both double-aluminized and double-siliverized mylar radiation barriers was computed for the two missions. The weight penalty is taken as the sum of the boiloff weight during the storage period and the weights of all the elements of the insulation system.

Details concerning the analyses and results of this configuration trade-off study are given in Sections 3.0 and 4.0.

3.0 ANALYTIC TECHNIQUES

3.1 Description of Computer Capabilities

Most of the HTTA thermal analysis and performance predictions were performed with the Thermal Analyzer Program (TAP) and Hydrogen Properties Program (PRHYD) which operate on the Beech IBM 360 Computer. TAP uses a "lumped parameter" finite-difference method to perform transient and steady-state solutions for a wide variety of thermal problems involving conduction, radiation, convection, and fluid flow. Convergence of steady-state solutions is determined by temperature fluctuations between successive iterations and by an overall energy balance. PRHYD computes hydrogen thermodynamic properties and functions needed to compute fluid expulsion rates from the pressure vessel, and uses a simplified thermal model to compute heat leaks and determine time histories of fluid storage conditions.

3.2 Thermal Network Models

TAP was used to compute constant-pressure boiloff rates for the three vapor-cooling configurations which were considered in the configuration

trade-off study. A simplified thermal network model in which the vapor-cooled shield and boiler shield were considered to be isothermal was used for this purpose.

A more sophisticated model was constructed in order to make performance predictions for the final HTTA insulation configuration. Spot checks revealed good agreement between the results obtained with the simplified and more sophisticated models.

In all cases analyzed the thermal conductivities of the pressure vessel support bands and plumbing and the specific heat of the boiloff vapor were considered to be temperature dependent.

Detailed descriptions of these thermal models are contained in the two following sections:

3.2.1 Thermal Models for Configuration Trade-Off Study

The thermal network models used to compute constant-pressure boiloff rates for the configuration trade-off study are shown below. The three vapor-cooling configurations are: (1) vapor-cooled shield only, (2) vapor-cooled shield with complete boiler shield, and (3) vapor-cooled shield with boiler shield on cylindrical portion of vessel only. In the nodal networks below, R = radiation, K1 = conduction through pressure vessel support bands, K2 = conduction through fill and vent lines, and K3 = conduction through the vapor-cooled shield (and boiler shield) supports to the pressure vessel. Because of the sparsity of pressure vessel support bands, the vapor-cooled shield and boiler shield may be supported with nylon struts which are attached to the pressure vessel.

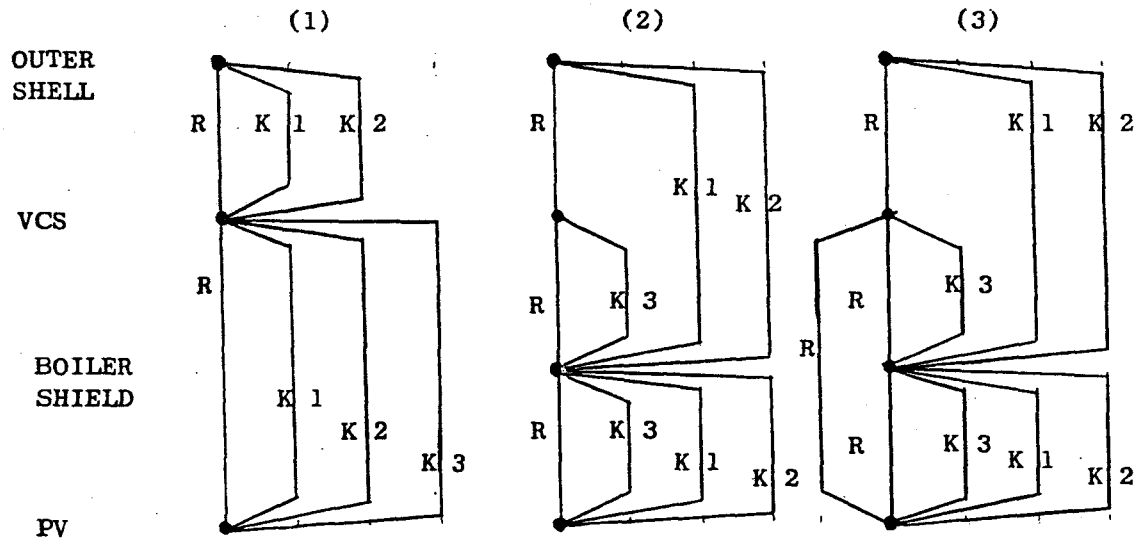

The pressure vessel support bands and the fill and vent tubes are thermally shorted to the boiler shield or to the vapor-cooled shield so that during operation with liquid venting, the conduction heat leak is absorbed before it enters the pressure vessel by the vented liquid. For configuration (1) the conduction members are shorted at locations halfway between the outer shell and pressure vessel to the vapor-cooled shield. For configurations (2) and (3) the support bands are shorted to the boiler shield at locations three inches from their attachment to the pressure vessel. For configurations (2) and (3), the fill and vent tubes are shorted to the boiler shield at locations 10 inches and 65 inches from their penetration into the pressure vessel, respectively.

The temperature-dependent thermal conductivities which were used for the stainless steel tubes and the composite glass bands are shown in Figure 2. Based on these curves, TAP was used to compute effective thermal conductivities for sections with one end fixed at 40, 540, and 600°R and with the temperature of the other end varying. These effective thermal conductivities were then used to compute the heat conduction between the pressure vessel and the thermal shorts and between the thermal shorts and the outer shell. Curves of effective thermal conductivity versus end temperature are shown in Figures 3 and 4 for stainless steel and composite glass bands, respectively.

Geometric inputs to the thermal models are as follows:

Plumbing - two stainless steel tubes, 2.5" O.D. x 0.028" wall x 130" long.

Pressure Vessel Support Bands - filament-wound glass, 0.12 in^2 cross-sectional area (each band), 16 bands - 27" long, 6 bands - 18.6" long.

Vapor-Cooled Shield Supports - nylon (thermal conductivity = 0.1 Btu/ft-hr-°R), 0.05 in^2 cross-sectional area (each support), 2.50" long (vapor-cooled shield and boiler shield are both supported with same support struts), total of fifty supports.

Radiation Areas:

Outer shell to vapor-cooled shield:	552 ft^2
Vapor-cooled shield to boiler shield:	506 ft^2
Vapor-cooled shield to pressure vessel:	502 ft^2
Boiler shield to pressure vessel:	488 ft^2

Radiation heat transfer in the thermal network model is computed by $Q_R = \epsilon_{eff} \sigma A(T_H^4 - T_C^4)$. All geometric view factors were considered to be unity for this study.

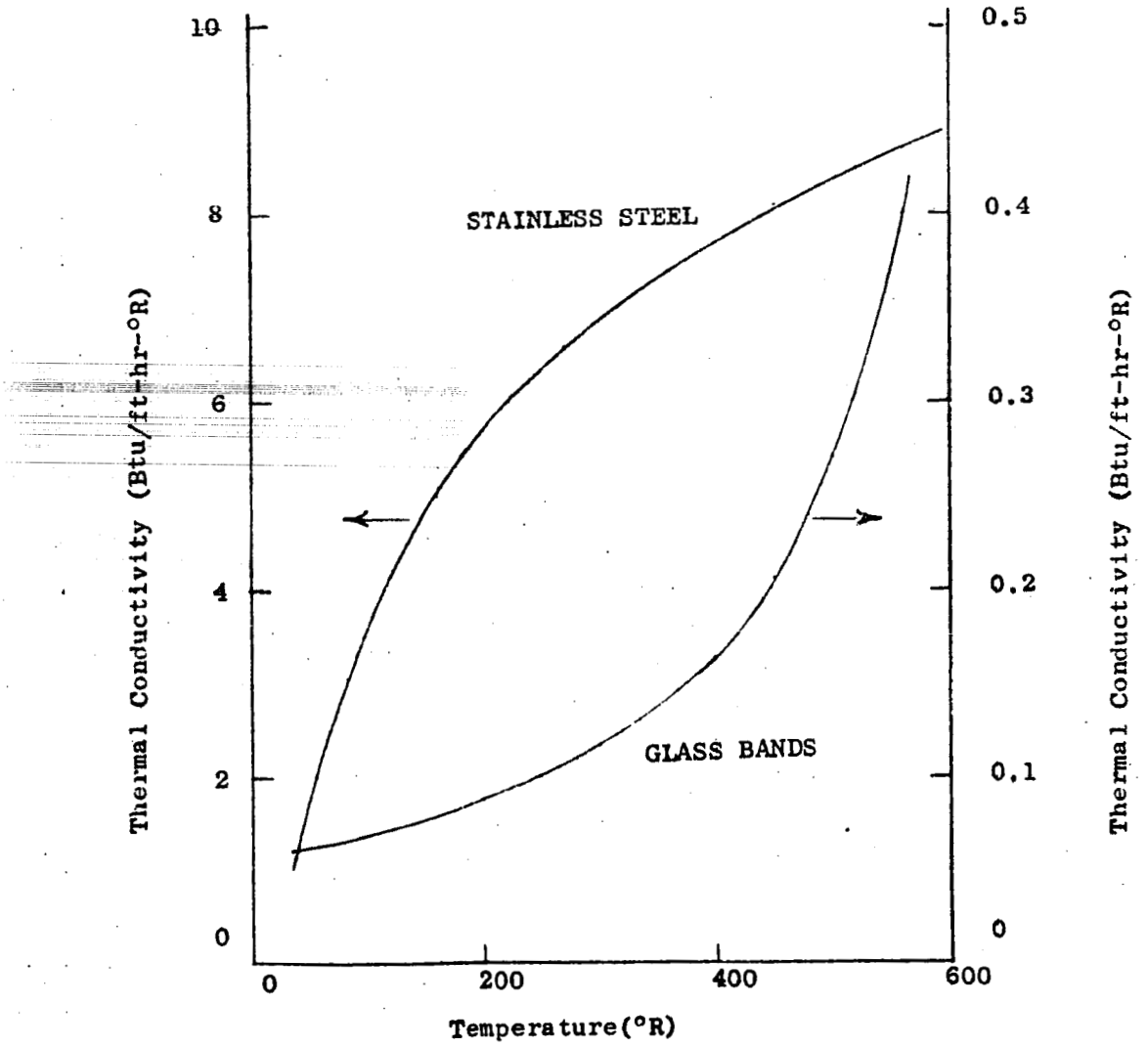

Figure 2 - Thermal Conductivities of Stainless Steel and Filament-Wound Glass Bands.

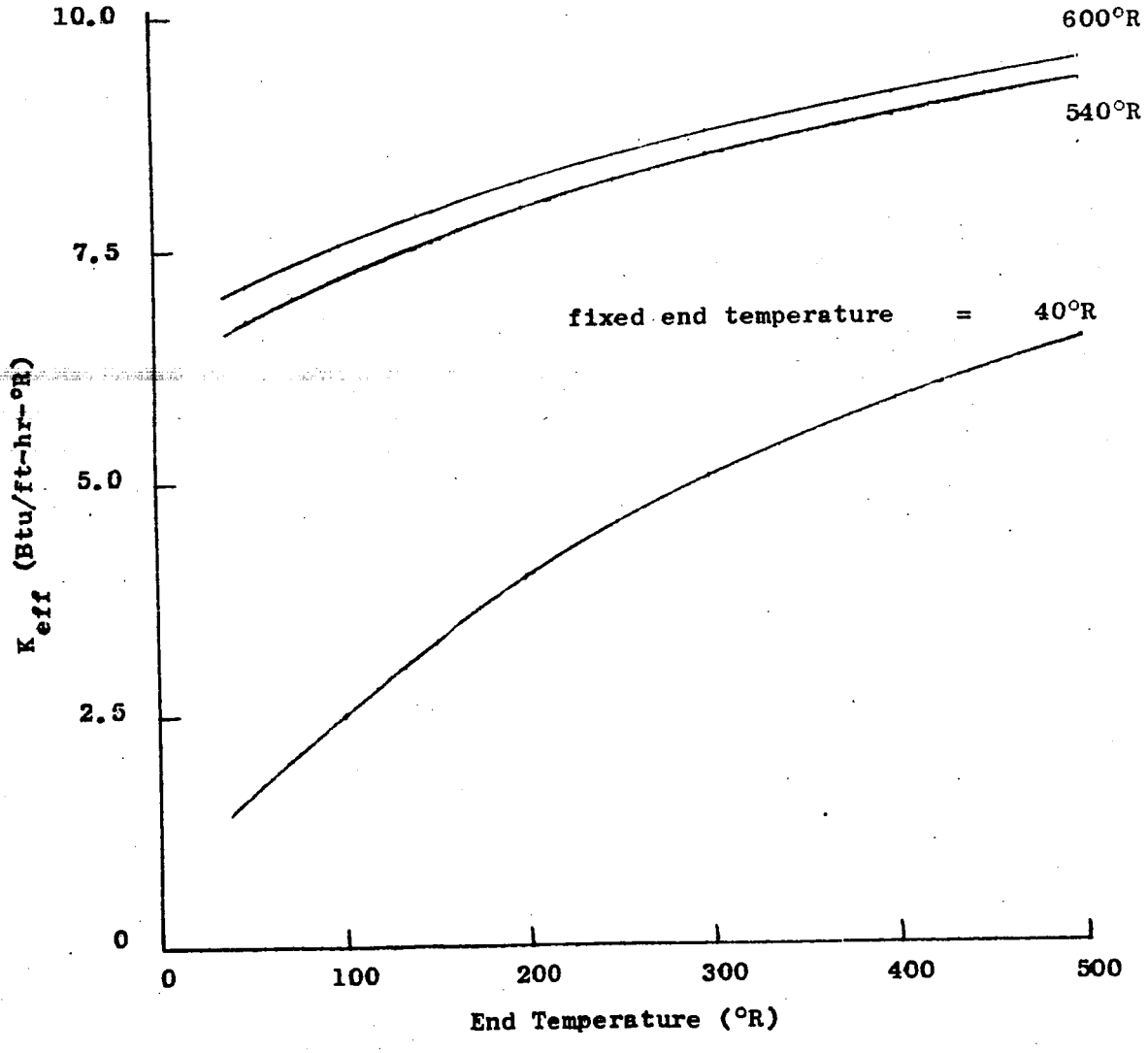

FIGURE 3 -

Effective Conductivity of Stainless Steel

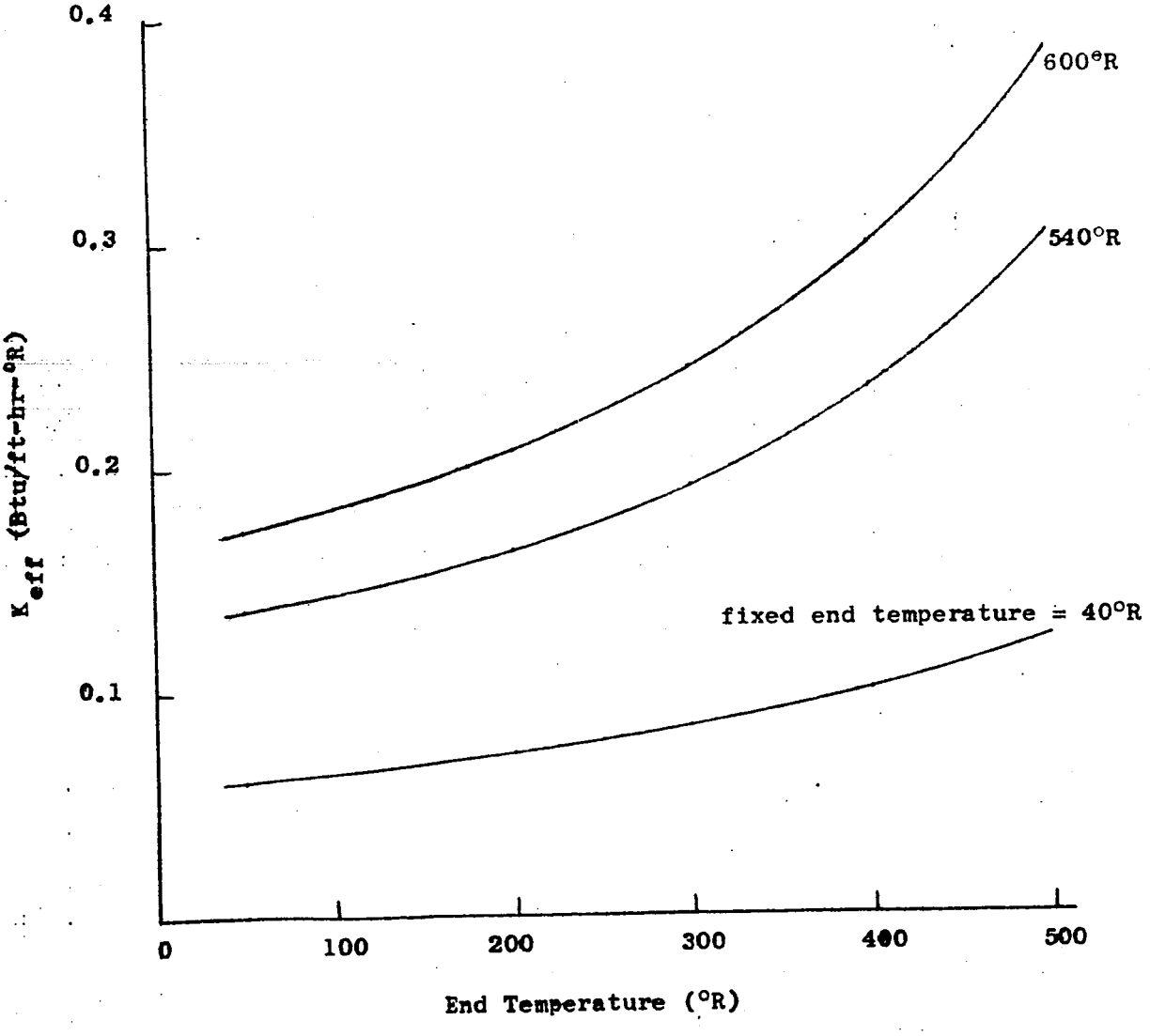

FIGURE 4 -

Effective Conductivity of Filament-Wound Glass Bands

The relationships between effective emittance and number of multilayer insulation barriers were obtained from Equations (4.22) and (4.38) of Reference 2 for this configuration trade-off study (see Section 4.2). Equation (4.22) is based on test data with double-aluminized mylar and double-silk net spacer, and Equation (4.38) is based on test data with double-goldized mylar and double-silk net spacer. It is assumed that the emittance characteristics of silverized and goldized mylar are similar enough that Equation (4.38) is applicable for this study (i.e., for determining optimum number of multilayer insulation barriers and associated weight penalties).

Equations (4.22) and (4.38) include conduction terms which become significant for layer densities of approximately 30 and 20 layers per inch for double-aluminized mylar and double-silverized mylar, respectively. For determining layer densities the boiler shield, vapor-cooled shield, and outer shell were considered to be 0.5", 2.5", and 6.5" from the pressure vessel, respectively.

Vapor cooling is accounted for in the thermal models as follows:

Vapor Vented from Pressure Vessel:

Configuration 1 - An amount of heat equal to $\dot{m}\ (H_{VCS} - H_{PV})$ is removed from the vapor-cooled shield node.

Configurations 2 and 3 - An amount of heat equal to $\dot{m}\ (H_{BS} - H_{PV})$ is removed from the boiler shield node, and an amount equal to $\dot{m}\ (H_{VCS} - H_{BS})$ is removed from the vapor-cooled shield node.

Liquid Vented from Pressure Vessel:

Configuration 1 - An amount of heat equal to $\dot{m}\ (H_{VCS} - H_{PV} + H_V)$ is removed from the vapor-cooled shield node.

Configuration 2 - An amount of heat equal to $\dot{m}\ (H_{VCS} - H_{PV} + H_V)$ is removed from the boiler shield node, and an amount equal to $\dot{m}\ (H_{VCS} - H_{BS})$ is removed from the vapor-cooled shield node.

Configuration 3 - For the conditions analyzed, the boiler shield is not intercepting enough heat leak to vaporize all the liquid vented from the pressure vessel, and the boiler shield node will, consequently, be at liquid temperature. An amount of heat equal to $\dot{m}\ (H_{VCS} - H_{PV} + H_V) - Q_{BS}$ is removed from the vapor-cooled shield node.

$\dot{m}$ is computed as Q_{PV}/θ_V and Q_{PV}/θ_L for vapor and liquid vented from the pressure vessel, respectively. For this study thermodynamic properties were based on a pressure of 17 psia. Figure 5 contains curves of θ_V,

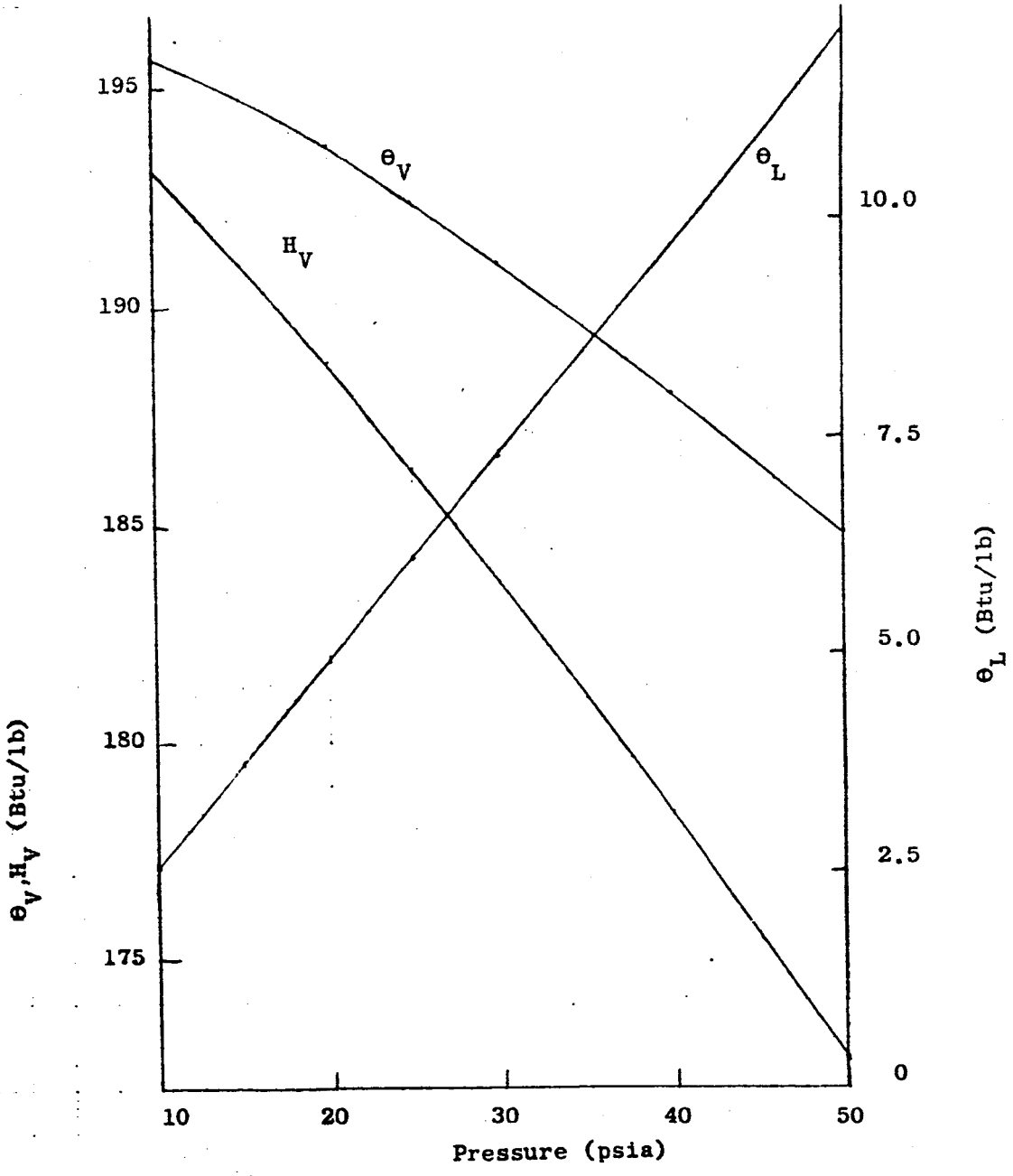

Figure 5 - θ_V, θ_L and H_V vs. Pressure for Saturated Liquid Hydrogen.

θ_L, and H_V versus pressure for saturated liquid hydrogen.

For configuration 4, boil-off rate was computed by:

$$\dot{m} = \left[\epsilon_{eff}\,\sigma\, A(T_{OS}^{4} - T_{PV}^{4}) + K(T_{OS} - T_{PV})\right] / \theta_V$$

where ϵ_{eff} was computed with Equations (4.22) and (4.38) of Reference 2, $A = 533\ ft^2$, and K is the effective conductance for the plumbing and pressure vessel support bands combined.

3.2.2 Thermal Model for Final Configuration Performance Predictions

A thermal network model which is more sophisticated than those described in the previous section will be used to predict performance of the chosen HTTA insulation configuration. The outer shell and pressure vessel will still be considered isothermal in this model.

The primary improvement in this model which provides more accurate and comprehensive results is that the boiler shield and vapor-cooled shield are each represented with a series of connected nodes. Each of these nodes represents a section of shield with attached tube and cooling vapor. Previous analyses and experimentation with the OTTA (Ref. 1) indicate that as few as 20 nodes provide accurate representation of a vapor-cooled shield. This is because the shields are for the greater part nearly isothermal.

Since the vapor-cooled shield and boiler shield are represented with a series of nodes, conduction elements of the insulation system can now be represented individually, and the locations of their attachments to the vapor-cooled shield and boiler shield can be approximately accounted for.

Fluid thermodynamic properties are considered temperature and pressure dependent, and all material thermal conductivities are considered temperature dependent.

A thermal network model for TAP utilization for a configuration consisting of a vapor-cooled shield with a complete boiler shield and the current plumbing and pressure vessel support system is shown in Figure 6.

Heat flows included in this model are (1) radiation from the outer shell to the vapor-cooled shields, from the vapor-cooled shield to the boiler shield, and from the boiler shield to the pressure vessel,

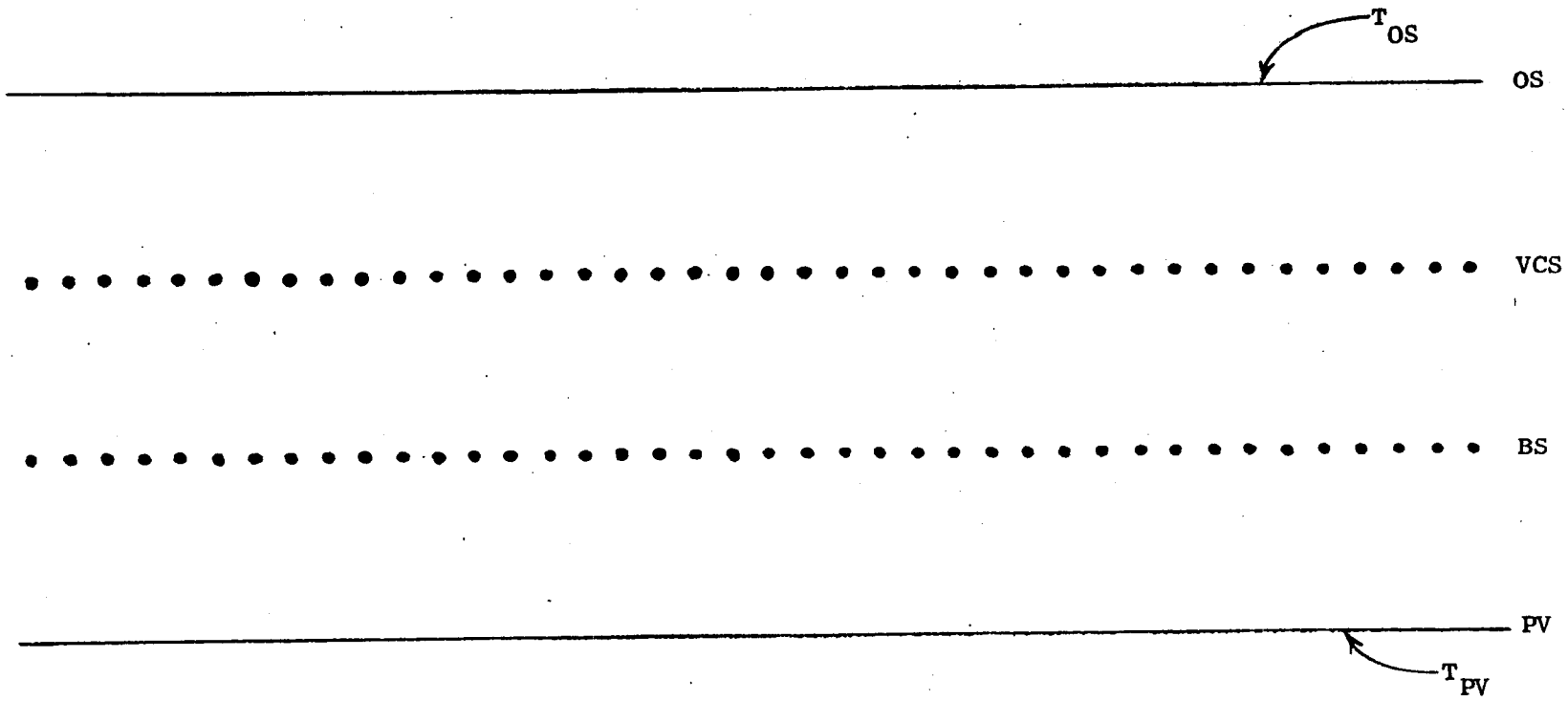

- OUTER SHELL AND PRESSURE VESSEL ASSUMED ISOTHERMAL
- MATERIAL AND FLUID PROPERTIES CONSIDERED TEMPERATURE DEPENDENT

FIGURE 6 - HTTA THERMAL NETWORK MODEL (VCS WITH COMPLETE BOILER SHIELD) contd

(2) conduction through the pressure vessel support system and plumbing, through the vapor-cooled shield and boiler shield supports, through the shorting straps between the plumbing and boiler shield, and in the vapor-cooled shield and boiler shield, and (3) absorption by heat flow. The thermal model will be updated to incorporate insulation system changes during HTTA design and development.

The multilayer insulation effectiveness is represented in the thermal model with a total blanket emittance (ϵ_{eff}) which depends on surface emittance, number of layers, penetration gaps and edge effects, spacer performance, compression effects and boundary temperatures. Evaluation of multilayer insulation performance is the largest source of inaccuracy in analytic predictions of thermal performance for cryogenic tankage. Needed values of ϵ_{eff} are determined from data in the literature, from company-funded experimental investigations with the Beech Insulation Comparator, and from estimates of layup degradation based on available data and Beech experience on Apollo (Reference 7), Lunar Module - LM (Reference 8), and OTTA (Reference 1) cryogenic tankage.

4.0 RESULTS OF CONFIGURATION TRADE-OFF STUDY

The analysis to determine the optimum placement of the vapor-cooled shield within the multilayer insulation is contained in the next section. The thermal network models shown in Section 3.2.1 were used to compute heat leaks and boil-off rates for the candidate vapor-cooling configurations using the determined optimum vapor-cooled shield location.

The results consist of curves of boil-off rate versus total effective emittance of the multilayer insulation for the four candidate configurations and for both vapor and liquid vented from the pressure vessel. Curves of total number of multilayer radiation barriers versus total effective emittance were generated for double-aluminized mylar and double-silverized mylar with double silk net. With these two sets of curves, combined insulation system and boil-off weight was determined as a function of total effective emittance. The minimum weight penalty and corresponding optimum number of layers of multilayer insulation were then determined for each configuration from this last set of curves.

4.1 Optimum Vapor-Cooled Shield Location

The optimum vapor-cooled shield location will be determined in terms of the ratio of the effective multilayer blanket emittance between the vapor-cooled shield and the pressure vessel (ϵ_2) and the effective blanket emittance between the outer shell and the vapor-cooled shield (ϵ_1). Only heat transfer by radiation will be considered in this

computation. The energy balance for the vapor-cooled shield is:

$$Q_{VCS} - Q_{PV} = \dot{m} \ (H_{VCS} - H_{PV}) \qquad (1)$$

where

$$\dot{m} = Q_{PV}/\theta$$

$$Q_{VCS} = \sigma \epsilon_1 A_1 (T_{OS}^4 - T_{VCS}^4),$$

$$Q_{PV} = \sigma \epsilon_2 A_2 (T_{VCS}^4 - T_{PV}^4),$$

$(H_{VCS} - H_{PV}) = C_P (T_{VCS} - T_{PV})$ with vapor vented from the pressure vessel, and

$(H_{VCS} - H_{PV}) = C_P (T_{VCS} - T_{PV}) + H_V$ with liquid vented from the pressure vessel.

In order to facilitate manipulation of these equations, enthalpy of the vapor at any temperature, T, is defined as $C_P T$.

Expanding and rearranging Equation (1) yields:

$$\epsilon_2/\epsilon_1 = \frac{A_1 (T_{OS}^4 - T_{VCS}^4) \ \theta}{A_2 (T_{VCS}^4 - T_{PV}^4) \ (\theta + C_P T_{VCS} - H_{PV})} \qquad (2)$$

where

$$\epsilon_2/\epsilon_1 = 2 \ \epsilon_2/(1 + A_2/A_1) \ \epsilon_T - A_1/A_2$$

The objective now is to minimize Q_{PV}. Using Equation (2) and assuming $T_{VCS}^4 \gg T_{PV}^4$ gives:

$$Q_{PV} = \frac{\sigma (A_1 + A_2) \epsilon_T}{2} \left[\frac{\theta (T_{OS}^4 - T_{VCS}^4)}{\theta + C_P T_{VCS} - H_{PV}} + T_{VCS}^4 \right]$$

$$= \sigma (A_1 + A_2) \epsilon_T \quad (B/C + D)/2 \qquad (3)$$

where

$$B = \theta (T_{OS}^4 - T_{VCS}^4)$$

$$C = \theta + C_P T_{VCS} - H_{PV}$$

$$D = T_{VCS}^4$$

Setting the derivative equal to zero in order to find the minimum gives:

$$\frac{dQ_{PV}}{dT_{VCS}} = \frac{d (\frac{B}{C} + D)}{dT_{VCS}} = 0, \text{ or}$$

$$\frac{1}{C} \frac{dB}{dT_{VCS}} - \frac{B}{C^2} \frac{dC}{dT_{VCS}} + \frac{dD}{dT_{VCS}} = 0 \qquad (4)$$

where

$$\frac{dB}{dT_{VCS}} = -4 \theta T_{VCS}^3$$

$$\frac{dC}{dT_{VCS}} = C_P \text{, and}$$

$$\frac{dD}{dT_{VCS}} = 4 T_{VCS}^3 .$$

Substituting into Equation (4) and rearranging gives:

$$(C_P/\theta)\ T_{VCS}^{\ 5} - (1.25 - 2\ H_{PV}/\theta)\ T_{VCS}^{\ 4}$$

$$+ \left[(H_{PV}/\theta)\ (1 - H_{PV}/\theta)\right]\ (\theta/C_P)\ T_{VCS}^{\ 3} = + T_{OS}^{\ 4}/4 \qquad (5)$$

This equation was solved for T_{VCS} with

C_P = 3.0 Btu/lb-$^{\circ}$R,

T_{OS} = 540°R and 600°R,

θ = 194.4 Btu/lb
H_{PV} = 120.0 Btu/lb
} vapor vented from pressure vessel, and

θ = 4.25 Btu/lb
H_{PV} = 70.0 Btu/lb
} liquid vented from pressure vessel.

Values of θ and H_V are based on a pressure of 17.0 psia. Values of C_P corresponding to the range of T_{VCS} resulting from solutions to Equation (5) varied from 2.62 to 3.12 Btu/lb-$^{\circ}$R. The assumed value of 3.0 Btu/lb-$^{\circ}$R is considered adequate for the purpose of this analysis.

Solving Equation (5) for T_{VCS} and using the results in Equation (2) gives:

ϵ_2/ϵ_1 = 3.82 - vapor vented from pressure vessel, 600°R

= 2.51 - liquid vented from pressure vessel, 600°R

= 3.87 - vapor vented from pressure vessel, 540°R

= 2.62 - liquid vented from pressure vessel, 540°R

Since the location of the vapor-cooled shield should be optimized for the worse case mode of operation (liquid vented from the pressure vessel), a value of $\epsilon_2/\epsilon_1 = 2.0$ was used in the configuration trade-off study. Because of the temperature dependence of the multilayer insulation reflectance characteristics, this means that approximately 75% of the insulation should be placed outside the vapor-cooled shield.

Notice that the optimum vapor-cooled shield location for a configuration with a boiler shield and a vapor-cooled shield with liquid vented from the pressure vessel is essentially the same as that for a configuration with a single vapor-cooled shield with vapor vented from the pressure vessel. This implies that a different vapor-cooled shield location should have been used for each vapor-cooling configuration and for each venting mode. Boil-off rates were computed for some specific cases for ϵ_2/ϵ_1 ranging between 2.0 and 4.0, and the boil-off rates differed by less than 2% over that range. It is consequently believed that the use of $\epsilon_2/\epsilon_1 = 2.0$ for all cases did not impair the validity of the trade-off study to any significant extent.

4.2 Performance of Multilayer Insulation

Figure 7 contains curves of total blanket effective emittance versus number of layers for both double-aluminized mylar and double-silverized mylar with double silk net spacer. These curves were computed with Equations (4.22) and (4.38) of Reference 2 for environmental temperatures of 540°R and 600°R. The values shown in Figure 7 are based on a 4-inch annulus between the outer shell and vapor-cooled shield, a 2-inch annulus between the vapor-cooled shield and pressure vessel, and a vapor-cooled shield temperature of 200°R. The use of a different vapor-cooled shield temperature would have little effect on the end results of the computation. For all cases considered in the configuration trade-off study, the vapor-cooled shield temperatures varied approximately between 200°R and 300°R.

Equations (4.22) and (4.38) of Reference 2 are:

$$(4.22)\quad q = \frac{7.46 \times 10^{-12} (\bar{N})^{3.56} (T_H^2 - T_C^2)}{2 (N + 1)} + \frac{1.1 \times 10^{-11} \epsilon_{TRA} (T_H^{4.67} - T_C^{4.67})}{N}$$

HTTA

* Heat Fluxes Computed with Eqs. (4.22) and (4.38) of NASA CR 72605
* MLI Spacer Material is Double Silk Net
* Annular Space Between Outer Shell and VCS = 4"
* Annular Space Between VCS and PV = 2"
* VCS Temperature = 200°R

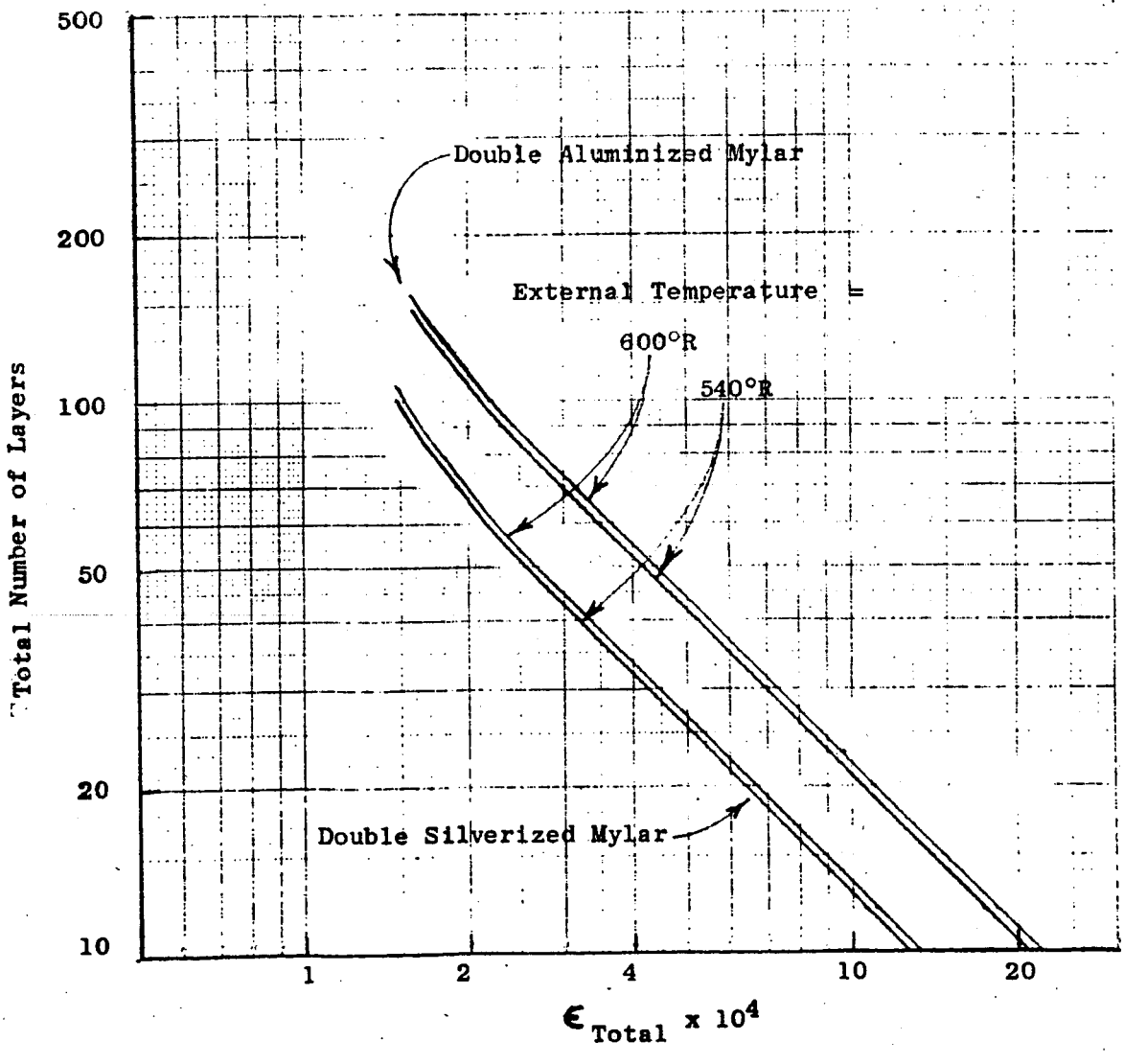

FIGURE 7 -

Number of MLI Barriers vs. Total Blanket Emittance

$$(4.38)\quad q = \frac{4.37 \times 10^{-11} \left(\bar{N}\right)^{3.27} \left(T_H^2 - T_C^2\right)}{2\left(\bar{N} + 1\right)} + \frac{6.7 \times 10^{-13} \epsilon_{TRS} \left(T_H^{4.51} - T_C^{4.51}\right)}{N \epsilon_{TRG}}$$

where

$\epsilon_{TRA} = 0.035,$

$\epsilon_{TRS} = 0.020,$

$\epsilon_{TRG} = 0.0215.$

Effective blanket emittance is defined as:

$$\epsilon_{eff} = q/\sigma \left(T_H^4 - T_C^4\right)$$

In order to account for multilayer insulation lay-up degradation effects (i.e., gaps around penetrations, edge effects, local compression), the right sides of Equations (4.22) and (4.38) were multiplied by 1.5 and 2.0 for the blankets above and below the vapor-cooled shield, respectively. The values of these degradation factors are based upon Beech's experience with previous cryogenic tankage.

The following steps were followed in generating Figure 7:

(1) Curves of effective emittance versus number of barriers were computed for the blanket above the vapor-cooled shield, for aluminized and silverized mylar, and for environmental temperatures of 540°R and 600°R.

(2) Curves of effective emittance versus number of barriers were computed for the blanket below the vapor-cooled shield for aluminized and silverized mylar.

(3) For a given total multilayer insulation emittance the emittances of the blankets above and below the vapor-cooled shield are defined ($\epsilon_2/\epsilon_1 = 2.0$), and the number of barriers above

Configuration
1. VCS Only.
2. VCS and complete boiler shield.
3. VCS and boiler shield on cylindrical portion only.
4. No vapor-cooling.

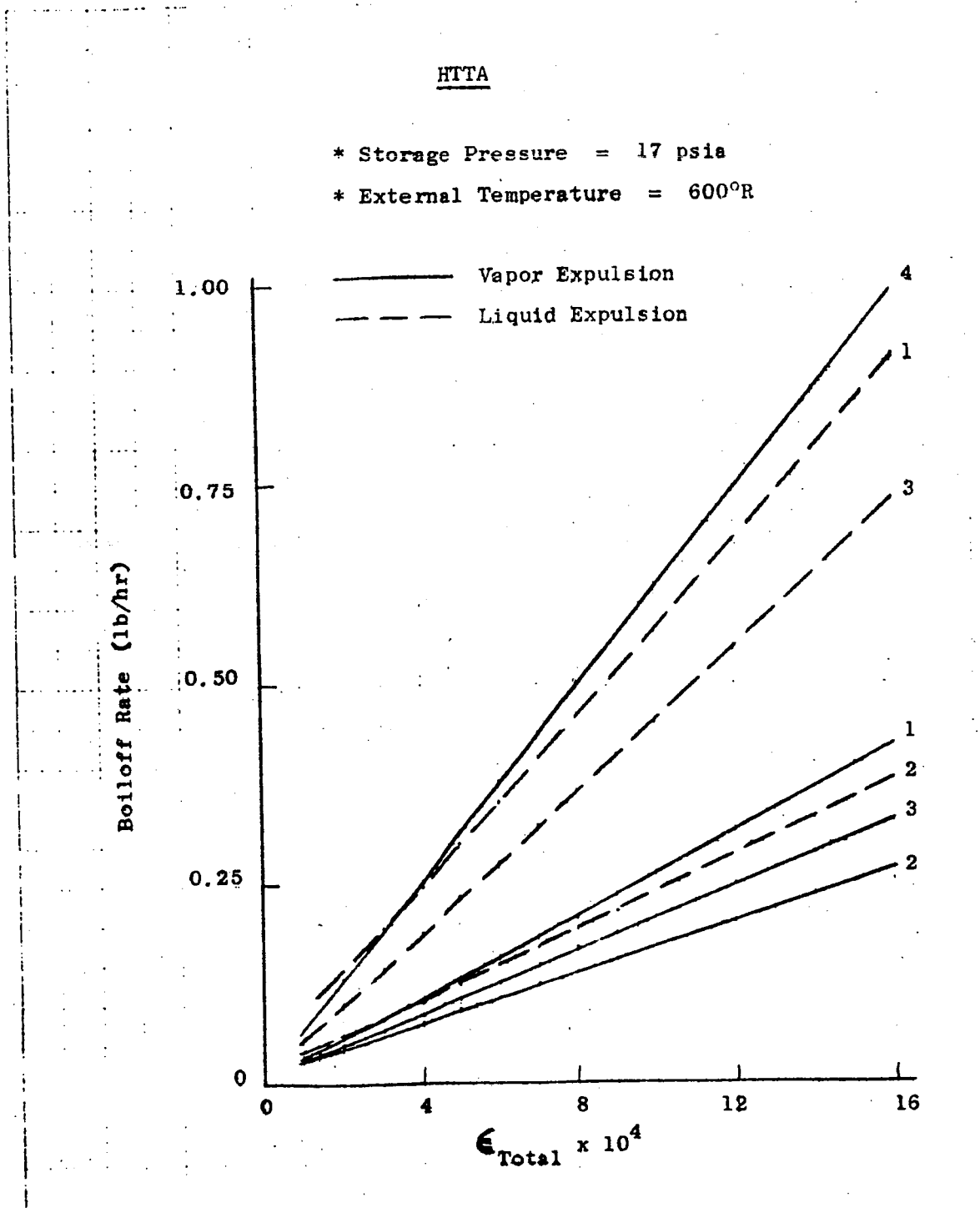

FIGURE 8

Boiloff Rate vs. MLI Total Emittance for External Temperature = 600°R (7-day Mission)

Configuration

1. VCS only.
2. VCS and complete boiler shield.
3. VCS and boiler shield on cylindrical portion only.
4. No vapor-cooling.

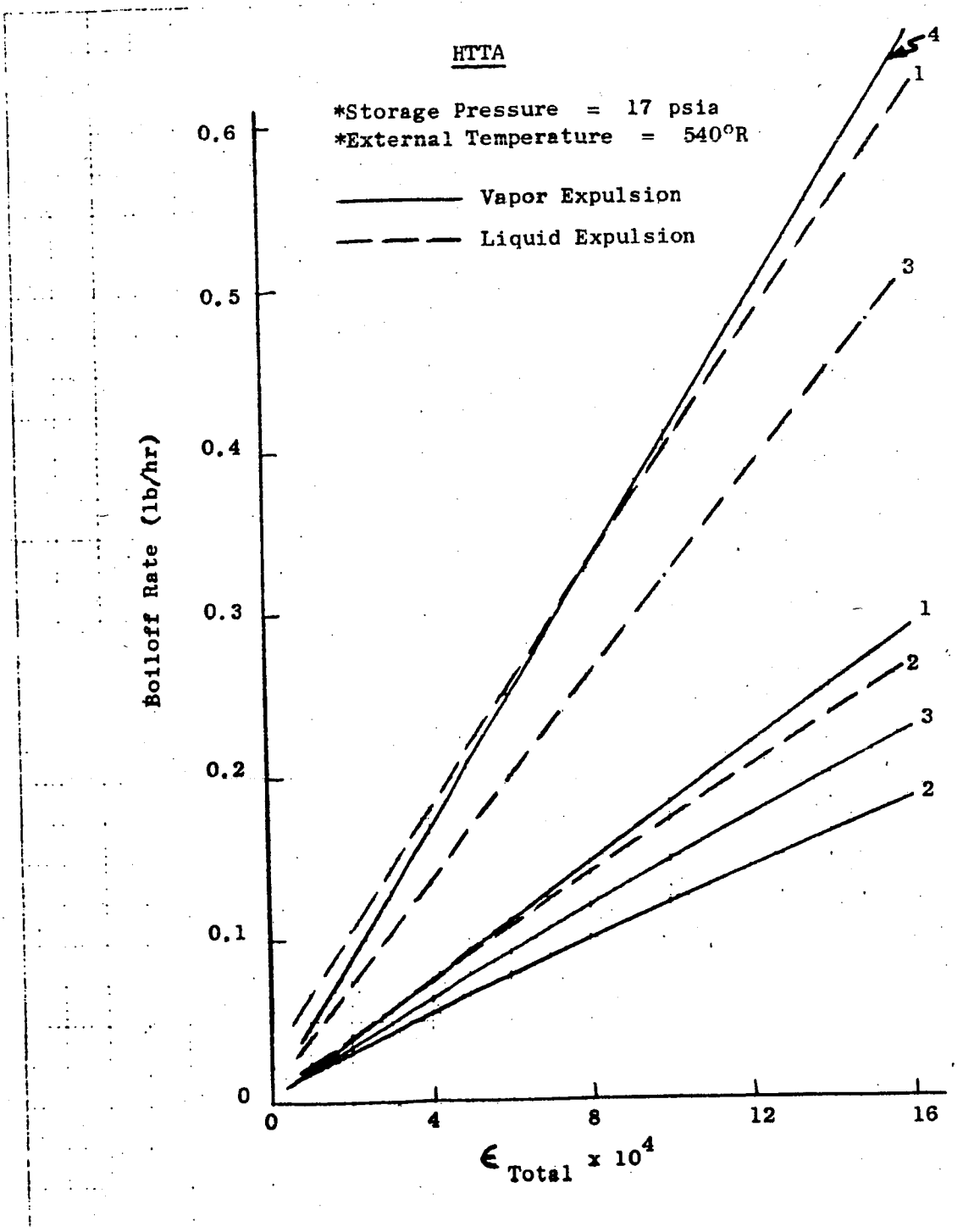

FIGURE 9

Boiloff Rate vs. MLI Total Emittance for External Temperature = 540°R (180-Day Mission)

and below the vapor-cooled shield can be obtained from the curves described above.

(4) Curves of total multilayer insulation emittance versus total number of radiation barriers can then be generated.

4.3 Configuration Selection for 7-Day and 180-Day Missions

Figures 8 and 9 contain curves of boil-off rates versus total multilayer insulation blanket emittance which were computed with the thermal network models described in Section 3.2.1 for the four vapor-cooling configurations listed in Section 2.5. Figures 8 and 9 correspond to environmental temperatures of 600°R and 540°R, respectively. Boil-off rates for both vapor and liquid vented from the pressure vessel are shown.

Shown in Figure 10 are curves of heat flux and total heat leak versus total multilayer insulation blanket emittance for operation in the vapor venting mode and for environmental temperatures of 540°R and 600°R.

Heat leaks and corresponding boil-off rates were computed for the effective blanket emittance between the vapor-cooled shield and pressure vessel (or boiler shield) being twice the value between the outer shell and vapor-cooled shield, as discussed in Section 4.1. The effective emittance between the vapor-cooled shield and pressure vessel (or boiler shield) is thus three times the total blanket emittance, and the value between the outer shell and vapor-cooled shield is 1.5 times the total blanket emittance. In cases with a boiler shield, it was assumed that two radiation barriers were present between the boiler shield and pressure vessel, and an effective blanket emittance of 0.01 was used.

Only vapor venting was considered for configuration 4 (no vapor cooling) because liquid venting would produce prohibitively high boil-off losses. It must consequently be assumed that a phase separating device is placed inside the pressure vessel in order to ensure vapor venting during zero-g operation. At present, the reliability of devices involving orifices or J-T valves is considered unacceptable for application to this tank. A passive retention device (screen) would be a more probable choice and would weigh between 100 and 200 pounds for a tank this size according to Reference 9. However, retention devices for this type of application are still in the development stage and flight-qualified hardware is not available. Since this tank will be used only for ground testing and can consequently be operated with either vapor or liquid vented from the pressure vessel, a phase separating device will not be installed.

Configurations

1. VCS Only.
2. VCS with complete boiler shield.
3. VCS with boiler shield on cylindrical portion only.
4. No vapor-cooling.

HTTA

* Storage Pressure = 17 psia

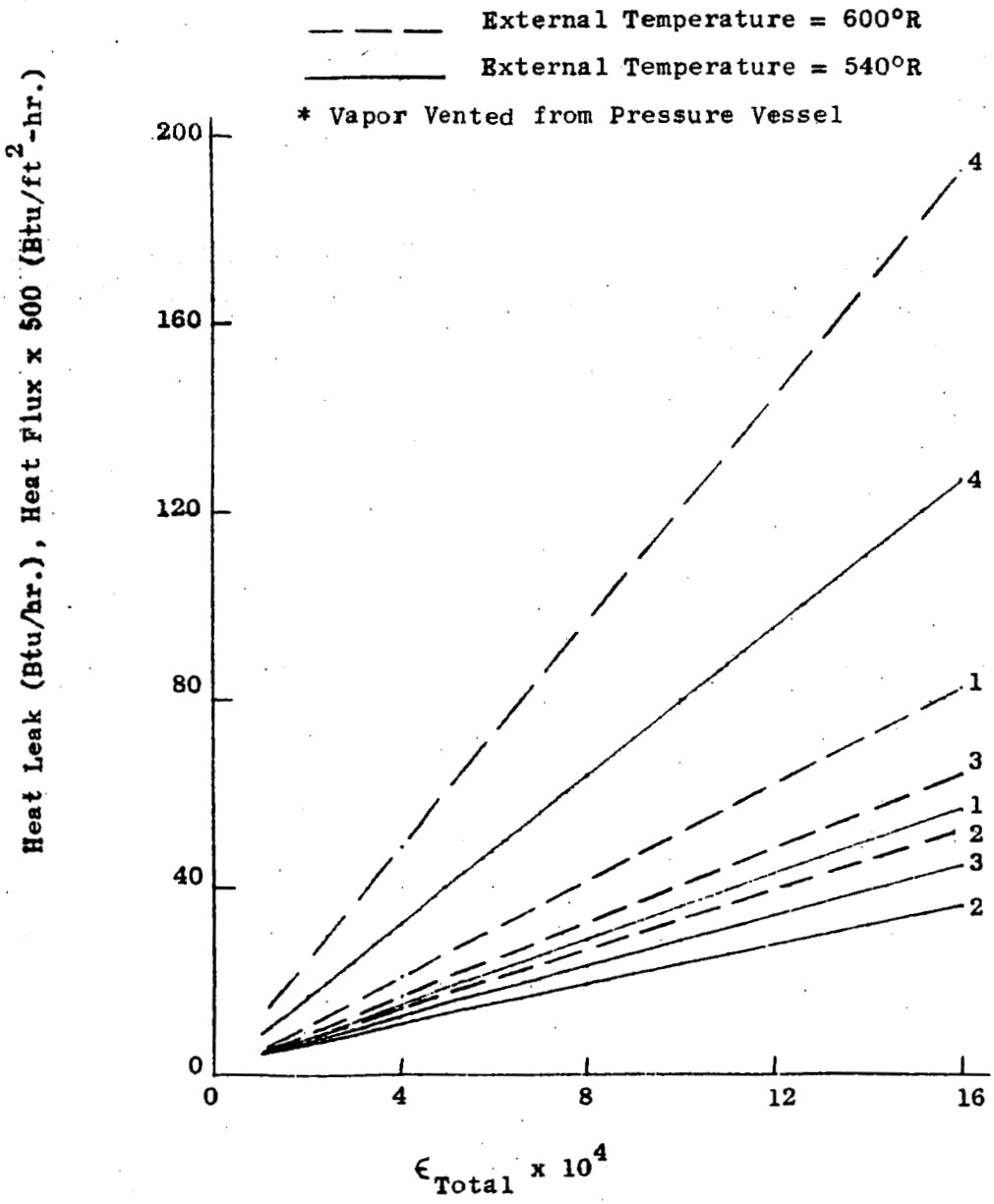

Figure 10 - Heat Flux and Total Heat Leak vs. MLI Total Emittance for Vapor Vented from Pressure Vessel

Figures 11, 12, 13, and 14 contain curves of combined boil-off plus insulation system weight versus total multilayer insulation emittance for 7-day storage with liquid venting, 7-day storage with vapor venting, 180-day storage with liquid venting, and 180-day storage with vapor venting, respectively. Weights which were used to construct these curves are:

(1) Vapor-cooled shield (0.008 inch thick) - 65 pounds.

(2) Boiler shield (0.008 inch thick) - 62 pounds.

(3) Cylindrical boiler shield - 37 pounds.

(4) Retention screen - 100 pounds.

(5) Multilayer insulation (1/4-mil mylar with either double silk net or single nylon net) - 2.3 lb/layer.

The number of multilayer insulation layers needed to produce the required blanket emittances were taken from Figure 7.

As mentioned in Section 2.3, single nylon net and double silk net appear to perform equally well as multilayer insulation spacer materials at higher temperature levels. The weights of the two can also be considered equal. Since two layers of silk cost a little over twice as much as one layer of nylon, it would be economically advantageous to consider a hybrid multilayer insulation system in which silk is used for the colder layers and nylon is used for the warmer layers.

During zero-g storage of a two-phase fluid without a phase separating device, the state of the fluid vented from the pressure vessel could be anything from pure vapor to pure liquid. Liquid venting is probable for the 180-day mission since the tank will be over 95 % full during the entire storage period. For the 7-day mission in which the tank will be approximately half full during the storage period (Figure 1), the fluid vented from the pressure vessel will probably be some combination of liquid and vapor. For purposes of selecting the minimum weight configurations, it is assumed that either a retention screen phase separator is employed or else liquid is vented from the pressure vessel.

The recommended insulation configurations based on the weight trade-off study with constant pressure operation and on the multilayer insulation selection discussed in Section 2.3 are:

Configuration

1. VCS only.
2. VCS and complete boiler shield.
3. VCS and boiler shield on cylindrical section only.
4. No vapor-cooling.

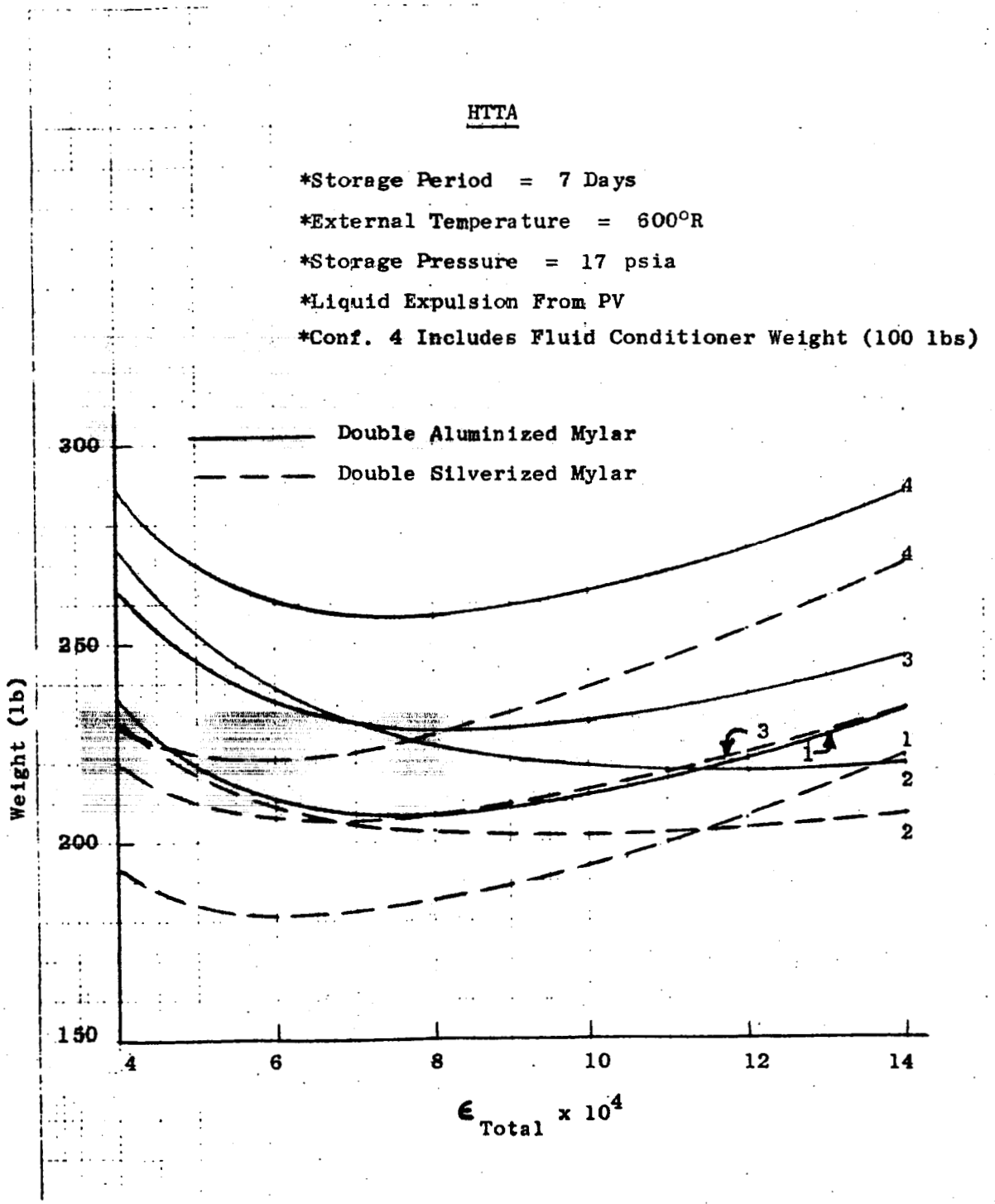

FIGURE 11-

Insulation System + Boiloff Weight vs. MLI
Total Emittance (7-Days, Liquid Expulsion)

Configuration

1. VCS only.
2. VCS and complete boiler shield.
3. VCS and boiler shield on cylindrical portion only.
4. No vapor-cooling.

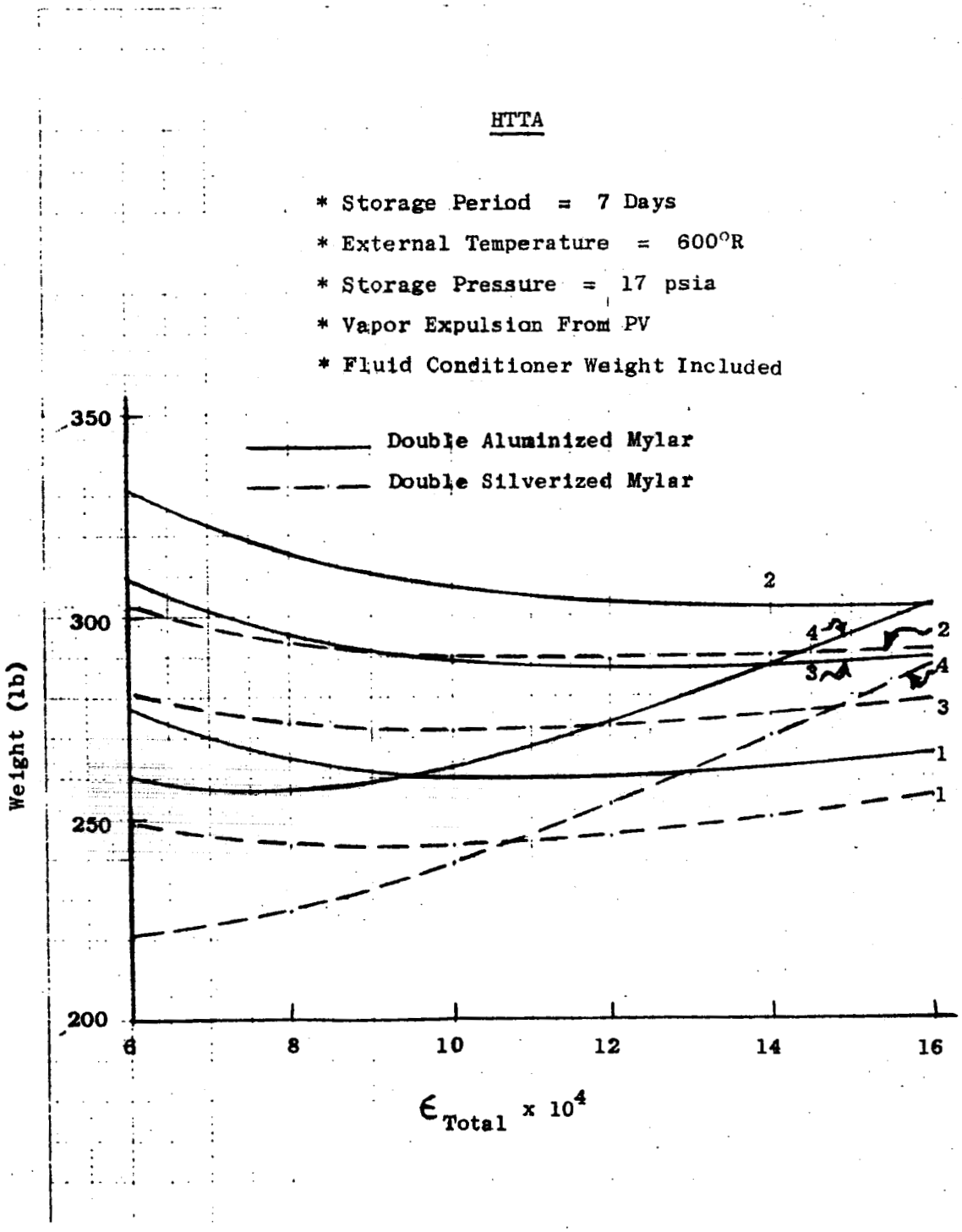

FIGURE 12 -

Insulation System + Boiloff Weight vs. MLI
Total Emittance (7-Days, Vapor Expulsion)

Configuration

1. VCS only.
2. VCS and complete boiler shield.
3. VCS and boiler shield on cylindrical portion only.

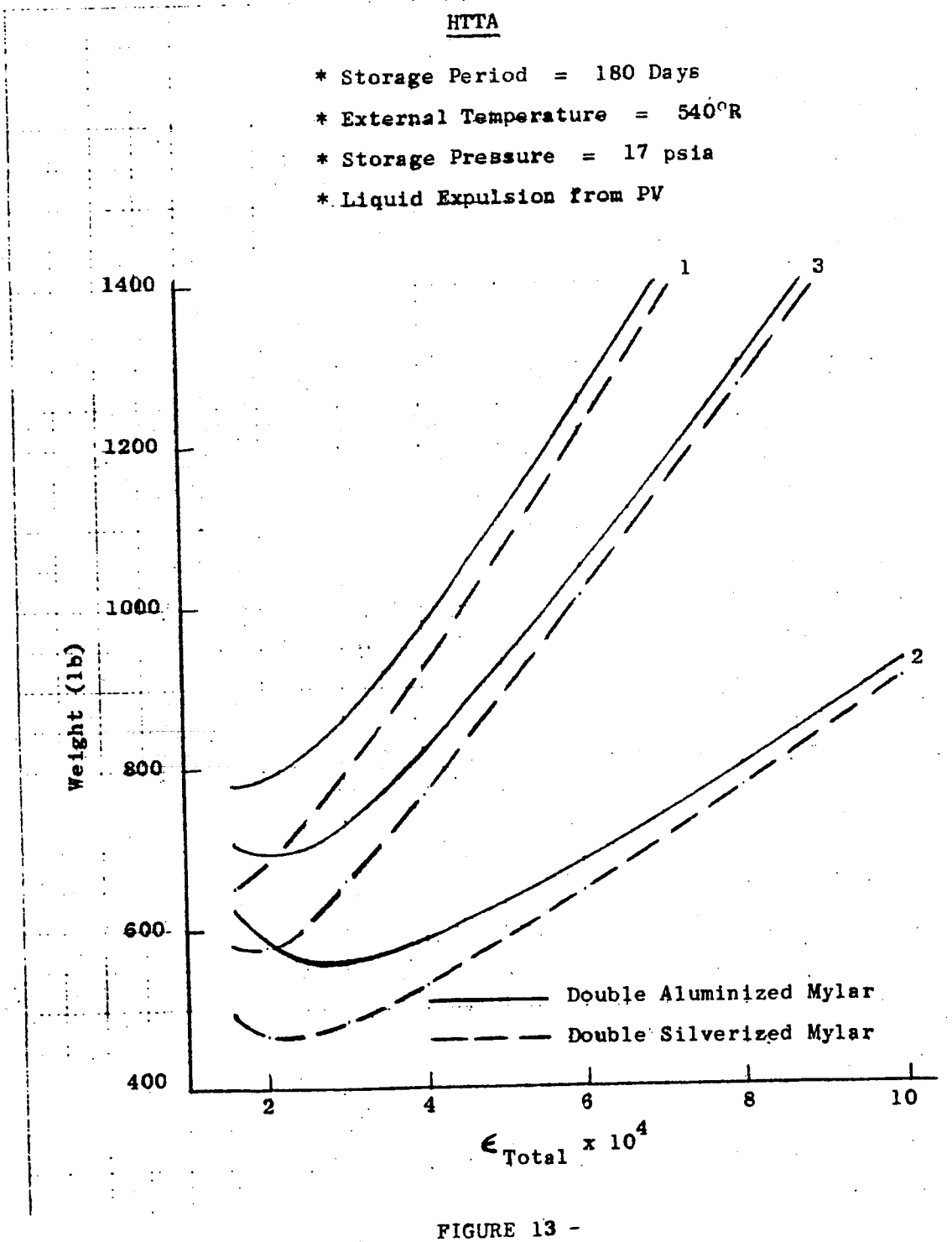

FIGURE 13 -

Insulation System + Boiloff Weight vs.
MLI Total Emittance (180-Days, Liquid Expulsion)

Configuration

1. VCS only.
2. VCS and complete boiler shield.
3. VCS and boiler shield on cylindrical portion only.

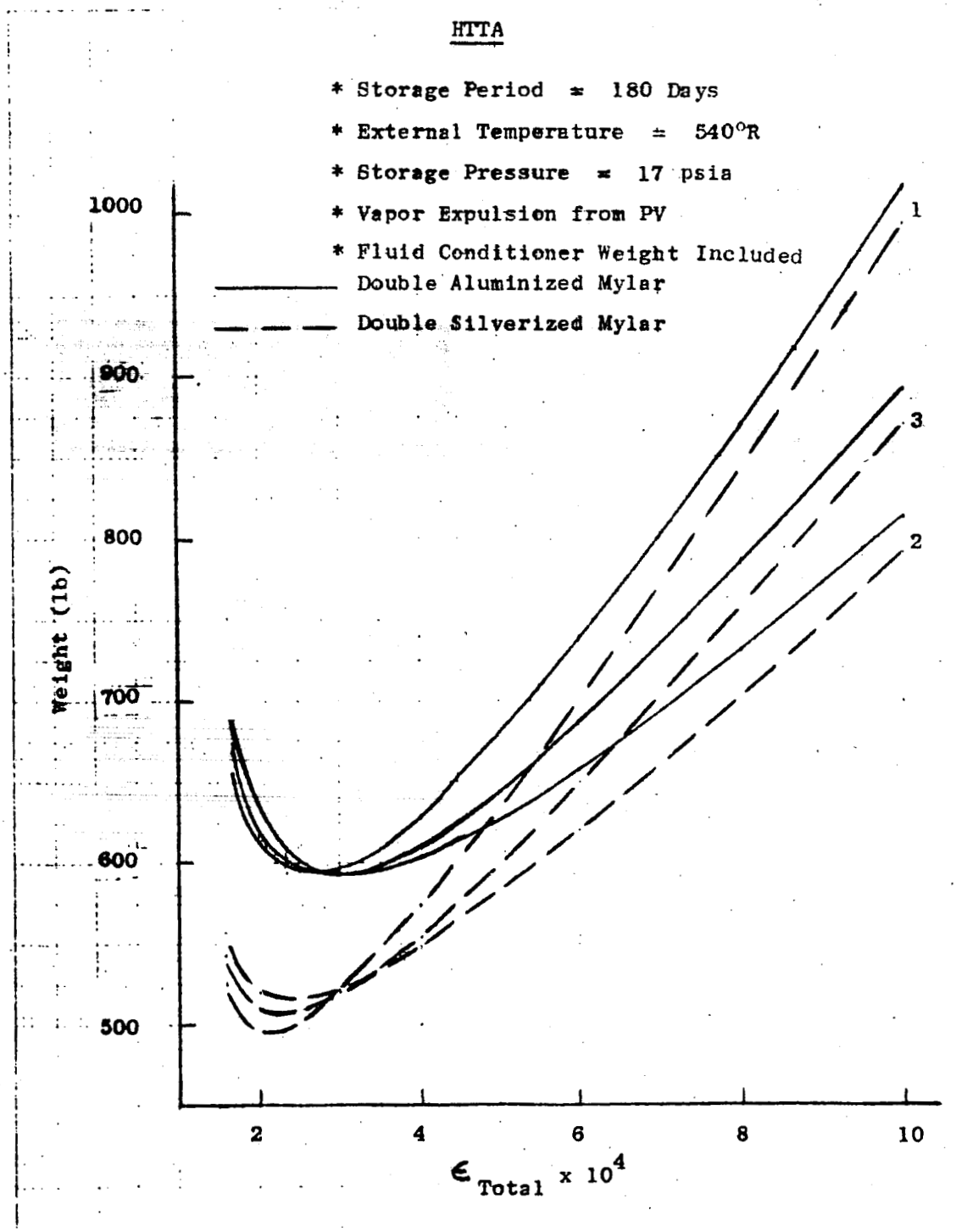

FIGURE 14

Insulation System + Boiloff Weight vs. MLI
Total Emittance (180-Days, Vapor Expulsion)

(1) 7-Day Mission:

*vapor-cooled shield only,

*no internal phase separator, and

*30 layers of multilayer insulation (aluminized mylar) -- 20 layers between the outer shell and vapor-cooled shield and 8 layers between the vapor-cooled shield and pressure vessel.

(2) 180-Day Mission:

*vapor-cooled shield with complete boiler shield,

*no internal phase separator, and

*68 layers multilayer insulation (silverized mylar) -- 46 layers between the outer shell and vapor-cooled shield, 20 layers between the vapor-cooled shield and boiler shield, and two layers between the boiler shield and pressure vessel.

It should be noted that aluminized mylar was chosen over silverized mylar for the 7-day mission because aluminized mylar is considered more durable and stable, which is important in consideration of the 7-day mission requirements. The use of silverized mylar would provide a weight savings of approximately 25 pounds. Based on Beech's experience to date with the OTTA (Reference 1), the reflective quality of silverized mylar is not degraded when proper storage and handling techniques are utilized prior to, during, and after installation. Surface reflectance measurements obtained by Beech indicate that moderate tarnishing does not significantly degrade the reflective quality of silverized mylar. Aluminized mylar is still the recommended material for the 7-day mission because of its superior reliability.

5.0 MULTILAYER INSULATION PERFORMANCE TESTING

Since radiation is the dominant mode of heat leak into this vessel, accurate predictions of thermal performance depend upon good estimates of the multilayer insulation performance. These estimates are obtained from flat plate test data, tank test data, and evaluation of layup degradation of the installed multilayer insulation.

For this study, estimates of layup degradation are based upon Beech's experience on Apollo, LM (Reference 8), and OTTA (Reference 1) cryogenic tankage. Experience and test data with OTTA are particularly valuable because of the similarity between OTTA and recommended HTTA multilayer insulation fabrication and layup techniques.

In-house testing is important in evaluating multilayer insulation performance because of (1) inconsistencies in testing and data reduction techniques which exist in information available in the literature, (2) lack of direct multilayer insulation performance comparison tests, and (3) lack of multilayer insulation performance data for the number of layers and boundary conditions desired.

5.1 Description of Apparatus

An apparatus (Beech Insulation Comparator) was designed and built at Beech-Boulder and has been in use for the past two years for thermal performance testing of multilayer insulations. As the name implies, this equipment was designed and is used primarily for comparing the thermal performance of different multilayer insulation materials. Before using the experimental data as an absolute measurement of insulation performance, heat losses through support elements and out the edges of the sample must be evaluated. These edge losses depend upon the test conditions and upon the sample being tested. The test apparatus has been designed to reduce these heat losses to a level such that they do not impair the validity of the equipment for comparing different insulation materials. The extent of edge losses has not been completely evaluated.

Figure 15 contains a description of the Beech Insulation Comparator and testing techniques. This apparatus has been used to evaluate the insulation characteristics of three multilayer insulations which are applicable to this program: (1) double-silverized mylar with double-silk net, (2) double-aluminized mylar with double-silk net, and (3) double-aluminized mylar with single-nylon net. Test results consist of heat fluxes through the multilayer insulation samples. These are then converted to effective emittances equivalent to those used in the thermal network models as explained in Section 3.0.

5.2 Results of Insulation Testing

Results of the multilayer insulation testing are shown in Figures 16, 17, and 18. Figure 16 contains results for samples consisting of 15, 25, and 40 layers of double-aluminized mylar with single-nylon net. Samples were tested with cold boundary temperatures of -115°F, -226°F, and -320°F and with hot boundary temperatures ranging up to 80°F.

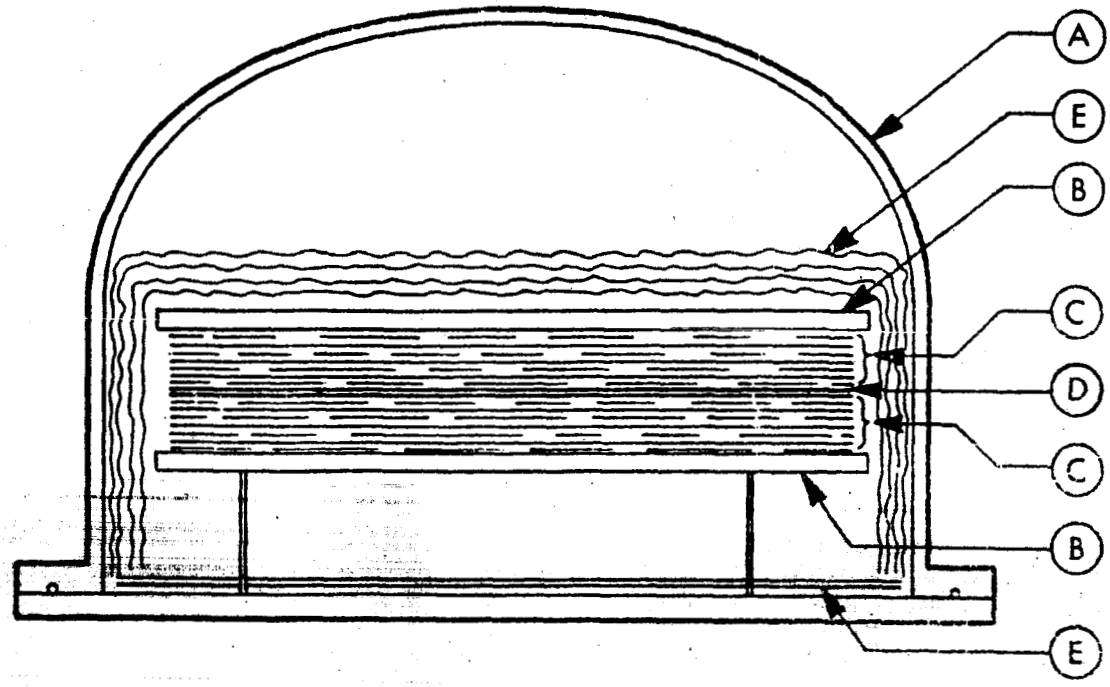

A. Vacuum Chamber - pressure level 1 x 10^{-7} torr.

B. Heat Sink (Cold Plate) - controlled temperature range: 320°F to 0°F

C. Insulation Sample - multilayer insulation layup.

D. Heater - three concentric heater elements temperature range ± 250°F.

E. Radiation Barrier - aluminized mylar shielding.

Circular insulation samples (C) are installed in exact layup configuration sandwiching thermally isolated heating elements (D). Thermostatically controlled "heat sink" plates (B) form the outside surface of the sample test sandwich. Centrally located insulation samples and heating elements are isolated from perimeter sections to eliminate "edge-effects" in the controlled sample area. Heating elements, cold plates, and radiation barriers are instrumented for temperature. Heat element input is controlled by vernier power supplies and recorded by digital voltmeters. The complete test bed is surrounded by multilayer radiation barriers and housed in a high vacuum chamber.

Figure 15 - Beech Insulation Comparator

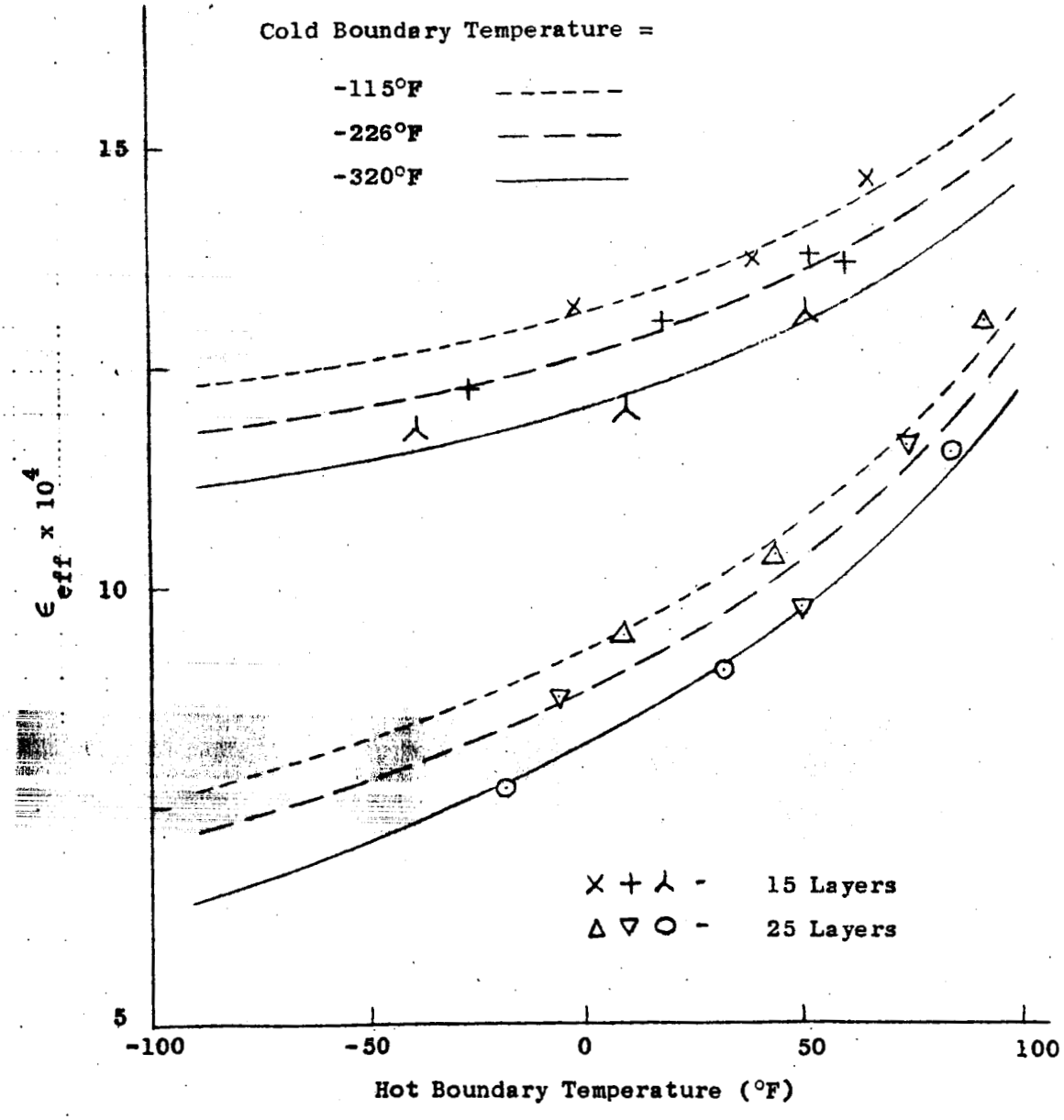

Figure 16 - Effective Blanket Emittance vs. Hot Boundary Temperature for 15 and 25 Layers of Double-Aluminized Mylar with Nylon Net Spacer

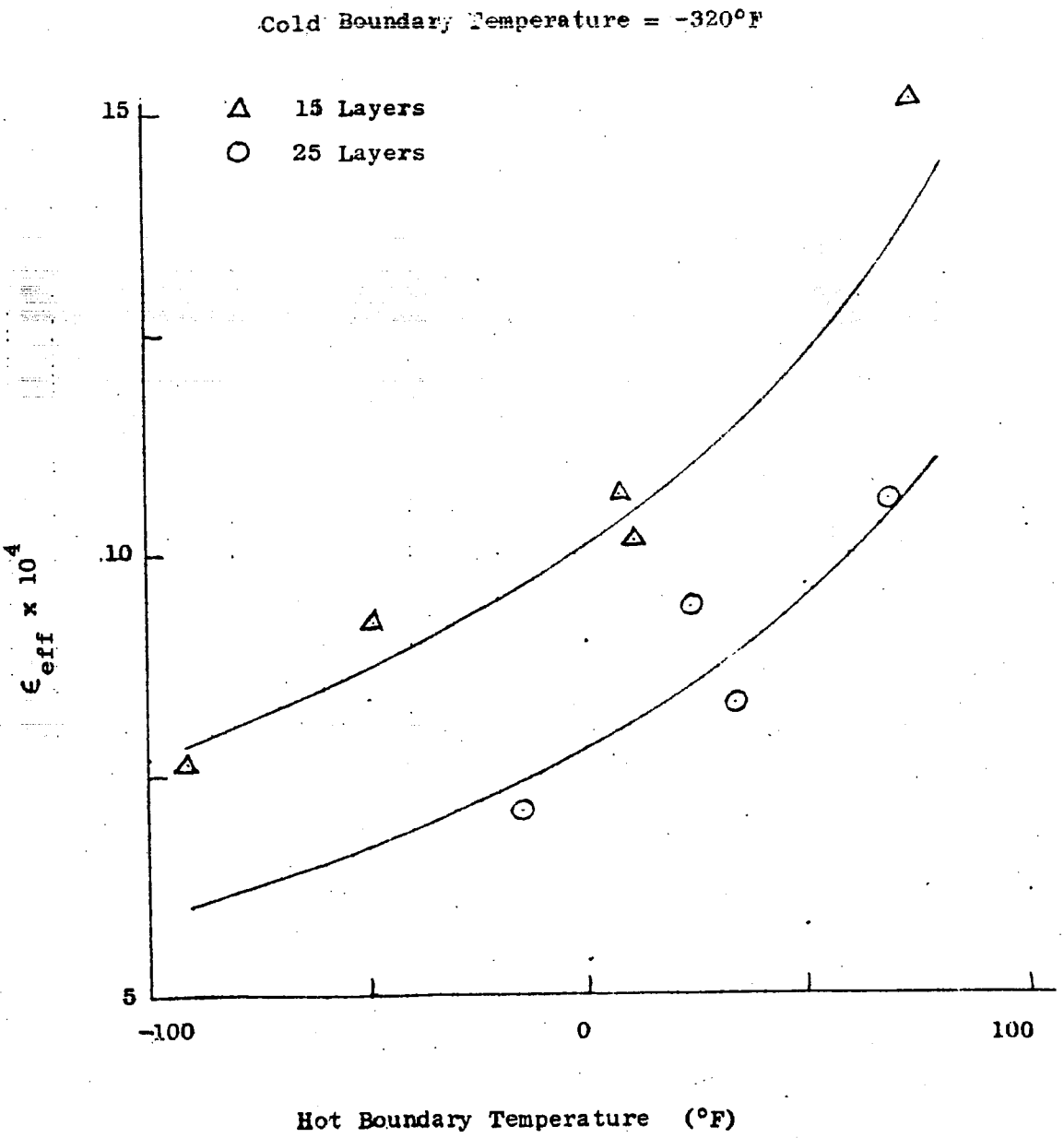

Figure 17 - Effective Blanket Emittance vs. Hot Boundary Temperature for 15 and 25 Layers of Double-Aluminized Mylar with Double Silk Net Spacer.

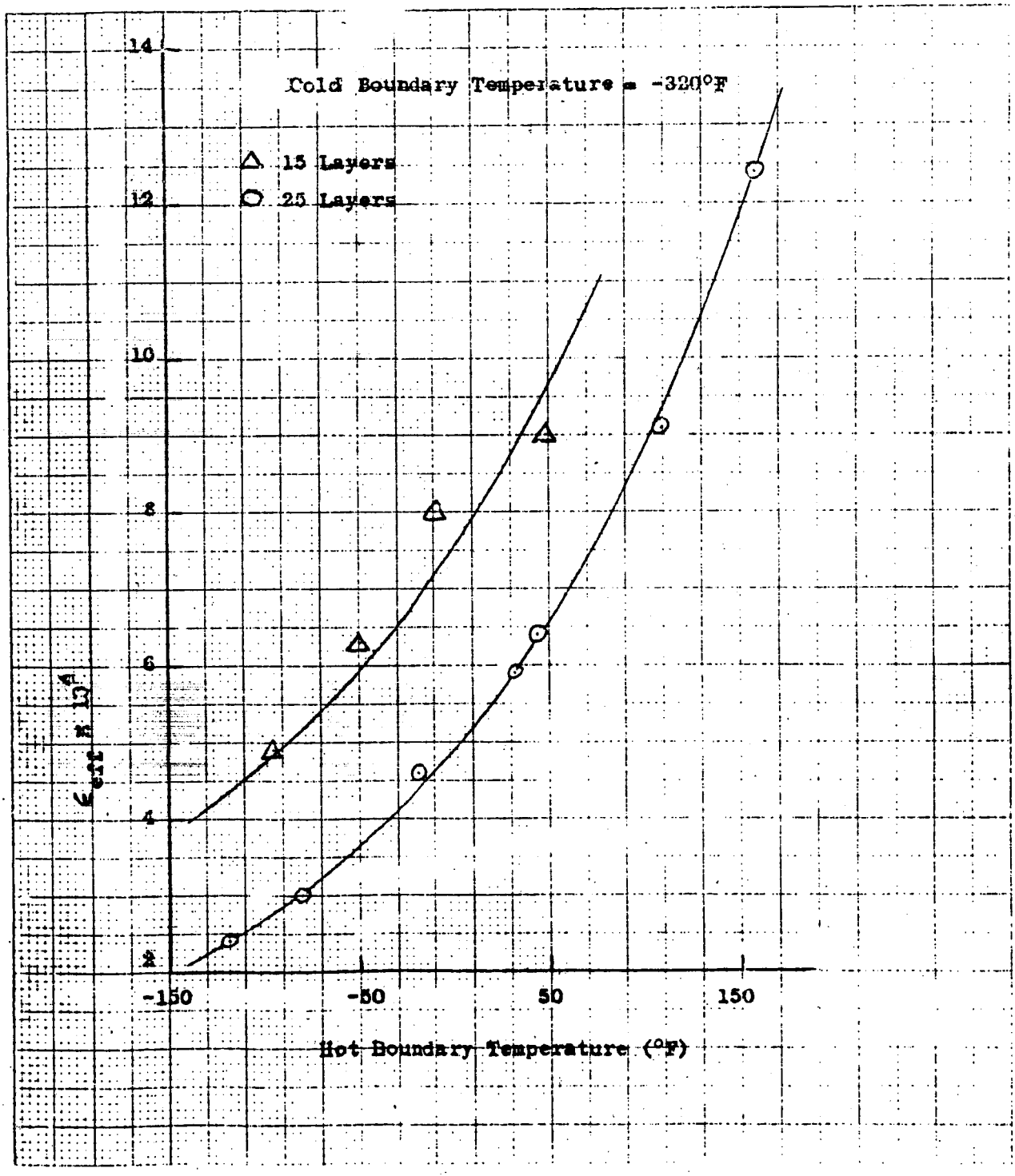

Figure 18 - Effective Blanket Emittance vs. Hot Boundary Temperature for 15 and 25 Layers of Double-Silverized Mylar with Double Silk Net Spacer.

Figure 17 contains results for samples consisting of 15 and 25 layers of double-aluminized mylar with double-silk net for a cold boundary temperature of -320°F. Figure 18 contains results for samples consisting of 15 and 25 layers of double-silverized mylar with double-silk net for a cold boundary temperature of -320°F.

Examination of Figures 16, 17, and 18 reveals that at the higher hot boundary temperatures, the effective emittances obtained increase more rapidly with increasing hot boundary temperature than should be expected. The only current explanation for this effect is that lateral conduction in the insulation samples becomes more noticeable at the higher temperature levels. When the sample loses heat out around the edges, more power is required in the heater plate to maintain the hot boundary temperature, and the effective emittance of the blanket appears to be higher than it actually is. It is felt that at this time the data obtained at higher temperatures should be interpreted with care. This problem will be examined more closely.

6.0 PERFORMANCE OF RECOMMENDED CONFIGURATIONS

6.1 Effect of Storage Pressure

Figure 19 contains curves of boil-off rates versus storage pressure for the two configurations recommended in Section 4.3 and for both vapor and liquid vented from the pressure vessel. These curves are based on constant pressure storage conditions where the liquid is saturated at the storage pressure.

Notice that the only case for which storage pressure has any significant effect upon boil-off rate over the range of pressure considered is the configuration with a vapor-cooled shield only and with liquid venting. This suggests that from a boil-off loss standpoint it would be advantageous to fill the tank with liquid at the highest possible saturation pressure. However, there is no overall weight advantage because the liquid density decreases as saturation pressure increases. The initial fluid mass in the tank consequently decreases as the saturation pressure of the fill fluid increases. This effect is shown in Figure 20 which contains curves of fluid mass remaining at the end of the mission versus storage pressure. Only mass loss due to boiloff is considered in this figure.

6.2 Pressure Rise without Venting

Optimum operation from the standpoint of minimizing fluid loss consists of allowing the liquid temperature (and pressure) to rise as long as the ullage space can accommodate the corresponding liquid expansion. This logic, of course, ignores the possible increase in pressure vessel weight caused by the higher operating pressure.

1 - External Temperature = 600°R,
30 Layers of DAM, VCS Only

2 - External Temperature = 540 R,
68 Layers of DSM, VCS and
Complete Boiler Shield

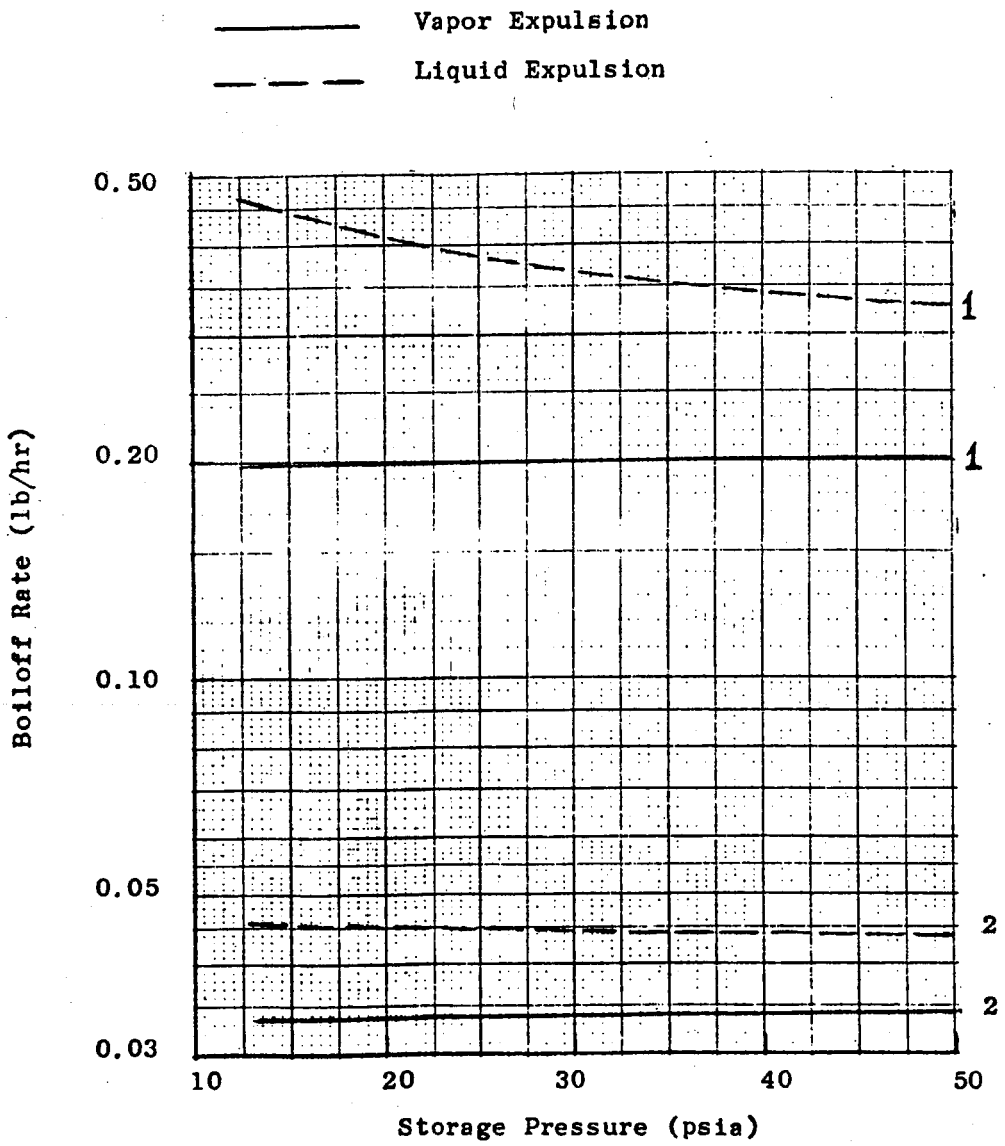

FIGURE 19 -

Boiloff Rate vs. Storage Pressure for
Weight-Optimized Configurations

1. 7-day mission, environmental temperature = 600°R, 30 layers of DAM, VCS only.

2. 180-day mission, environmental temperature = 540°R, 68 layers of DSM, VCS with complete boiler shield.

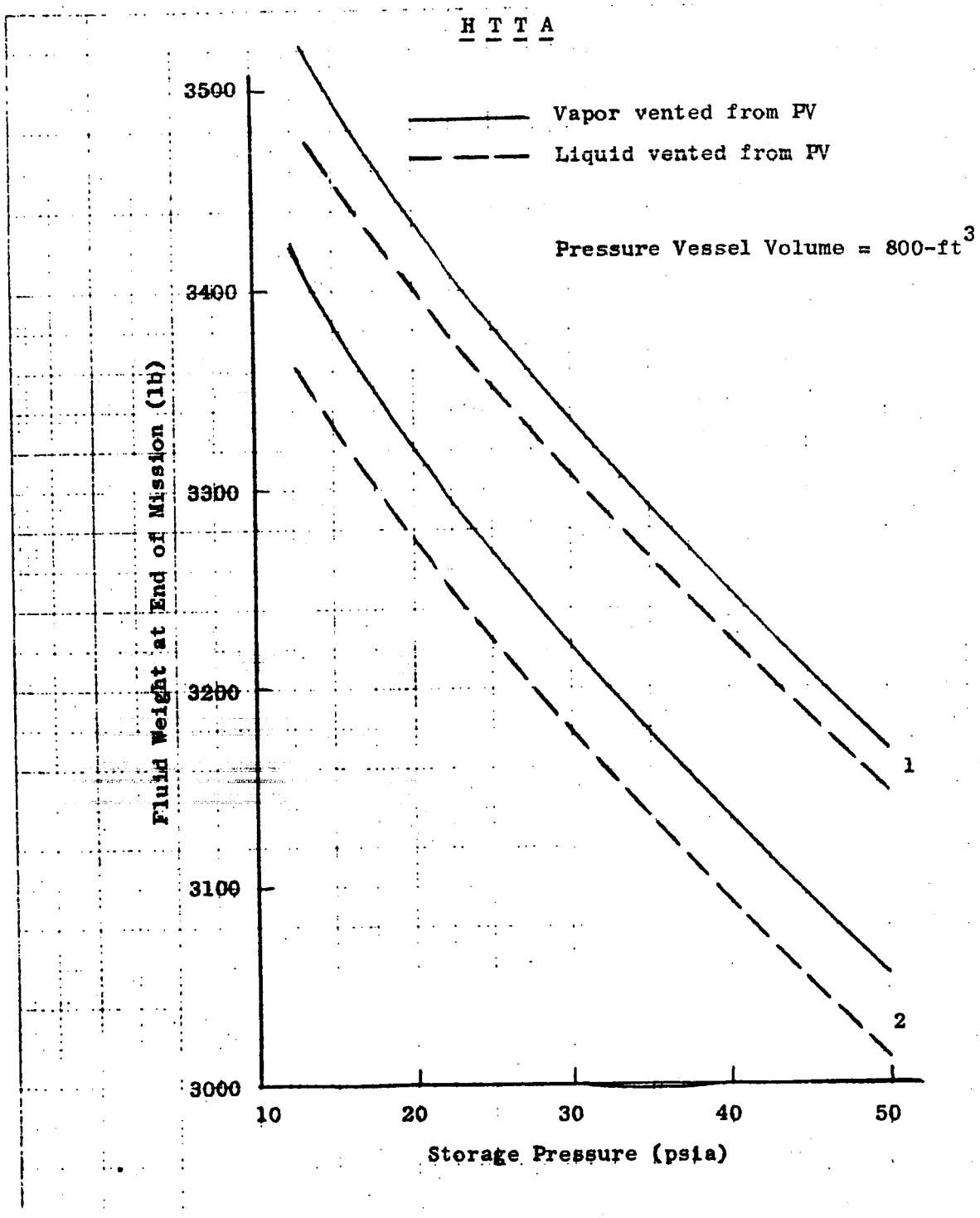

Figure 20 - Fluid Weight Remaining at End of Mission vs. Storage Pressure for Recommended Insulation Systems

Figure 21 contains curves of pressure versus time for the two recommended configurations for operation with no venting (i.e., no vapor cooling).

Because of the frequent fluid use associated with the 7-day mission and the likelihood that the fluid delivered to the pumps must be within a small range of saturation pressure, it is improbable that the liquid temperature (and saturation pressure) could be allowed to rise.

It is possible that significant weight savings could be realized by allowing the stored fluid to absorb some of the heat leak during the 180-day mission. However, this type of operation would require a more sophisticated and less reliable pressure control system, and the feasibility of such a system requires further investigation.

6.3 Effect of Fluid Quantity

Because of the small heat leak rates involved and the small resistance to heat flow laterally in the 0.16-inch thick aluminum walls of the pressure vessel, ullage size will have very little effect upon fluid boil-off rate. Effect of ullage size is of little interest for the 180-day mission since it is assumed that no fluid will be used during the 180-day storage period, and the ullage will consequently be no greater than 5%. Since the fluid quantity will be approximately 50% of a full tank for the 7-day mission, this case will be examined more closely in the following paragraphs.

Consider first the case where the tank is half full and in a one-g environment (testing). Assume that all the heat entering the pressure vessel in the region of the ullage must pass through the pressure vessel walls and into the liquid in the lower half of the tank. The heat leak to the pressure vessel during vapor venting operation will be much higher than during liquid venting operation and should thus be considered here in order to be conservative.

From Figure 11, the optimum total multilayer insulation effective emittance for aluminized mylar and liquid venting is 0.00075. From Figure 10, the corresponding total heat leak is 26.7 Btu/hr. Based on the assumption that one-fourth of this heat leak is conducted through a ten-foot length of the pressure vessel and into the liquid, then the temperature difference required from the top to the bottom of this ten-foot section is:

$$T = QL/kA$$

$$= \left(\frac{26.7}{4}\right)(10)/(60)\left(\frac{\pi}{144}\right)(45.5^2 - 45.34^2)$$

$$= 3.51^{\circ}R$$

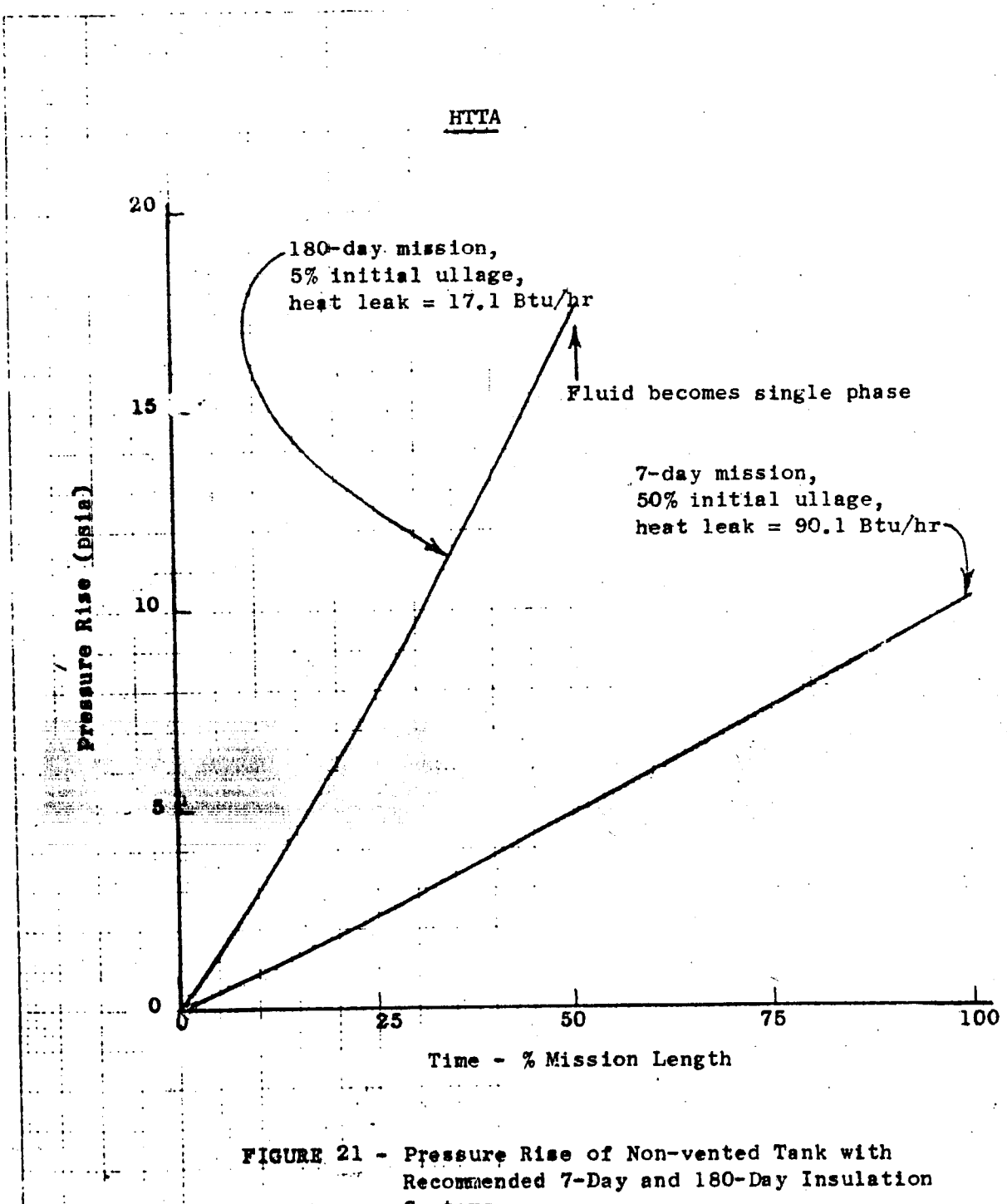

FIGURE 21 - Pressure Rise of Non-vented Tank with Recommended 7-Day and 180-Day Insulation Systems

This amount of temperature variation will have no significant effect upon the heat leak to the pressure vessel, and it can be concluded that the boil-off rate in a one-g environment is essentially independent of ullage size.

In a zero-g environment, the vapor will tend to collect around the walls of the pressure vessel. If anything, the boil-off rate will be reduced by this condition. A detailed analysis of this effect is beyond the scope of this study.

6.4 Effect of Stratification

Thermal stratification within the HTTA has been considered in order to determine its effects upon the thermal performance of the tank. The mechanisms of thermal stratification are complex, and a rigorous analysis to evaluate its effects is both tedious and difficult and could not be performed within the time and economical constraints of this study. Efforts were consequently directed toward a more qualitative evaluation of the possible effects upon the HTTA thermal performance during anticipated modes of operation.

A considerable number of analytical and experimental investigations of thermal stratification problems have been performed and reported in the literature. However, the available information generally pertains to specific tanks and configurations and cannot be readily applied to a reasonable estimate of the stratification effects within the HTTA.

The primary cause of thermal stratification is the lack of sufficient heat transfer mechanisms (conduction and convection) needed to distribute the incoming heat leak throughout the bulk of the fluid. The energy passing through the pressure vessel wall creates a warm boundary layer next to the wall. In a one-g environment the warm fluid in this boundary layer rises upward and is accumulated in a warm layer at the upper surface of the stored fluid.

If the tank was not vented during this process, the pressure rise measured in the ullage space would initially be greater than a non-stratified tank because the heat leak is absorbed by only a small portion of the stored fluid. However, after the warm layer forms on the liquid surface, the ullage pressure would tend to level off.

During vented operation where the ullage pressure is maintained at the saturation pressure of the fluid bulk, the warm fluid which is formed near the pressure vessel wall will rise to the surface and be boiled off. Because the heat flux incident upon the HTTA pressure vessel will be extremely small, it is expected that there will be no noticeable effect of thermal stratification upon the results of the constant pressure boil-off testing.

7.0 CONCLUSIONS AND RECOMMENDATIONS

A parametric study has been performed in order to determine optimum thermal protection systems for an 800-ft^3 subcritical hydrogen storage vessel for the Space Shuttle Orbital Maneuvering System 7-day mission and for a 180-day mission. Using the thermal performance and operational requirements of the two missions, insulation configurations were selected primarily on the basis of weight and reliability considerations.

For the 7-day mission the recommended system consists of a single vapor-cooled shield and double-aluminized mylar with double-silk net spacers in the colder layers and with single-nylon net spacers in the warmer layers. Based on the initial analyses, approximately 30 layers of multilayer insulation is weight optimized. Although silverized mylar is superior to aluminized mylar on a performance-to-weight basis, aluminized mylar was chosen for this mission because of its greater resistance to degradation when exposed to adverse conditions such as air, moisture, and abrasion.

For the 180-day mission the recommended system consists of a vapor-cooled shield with a complete boiler shield and double-silverized mylar with double-silk net spacers in the colder layers and with single-nylon net spacers in the warmer layers. Approximately 68 layers of multilayer insulation is weight optimized according to the initial analyses.

Estimated heat leaks and boil-off rates for the recommended insulation systems at a storage pressure of 17 psia are shown below.

	7-Day Mission	180-Day Mission
Boil-off Rate (Liquid Venting) - lb/hr	0.43	0.041
Boil-off Rate (Vapor Venting) - lb/hr	0.20	0.033
% Boiloff per Day (Liquid Venting)	0.293	0.028
% Boiloff per Day (Vapor Venting)	0.136	0.022
Heat Leak (Vapor Venting) - Btu/hr	39.0	6.40
Heat Flux (Vapor Venting) - Btu/ft^2-hr	0.078	0.013

A more sophisticated analytic technique than that used in the parametric study has been developed for predicting thermal performance characteristics of the installed insulation system. This analysis accounts for the operation of the insulation system in more detail and will incorporate more accurate estimates of the multilayer insulation effectiveness

than was done in the parametric study. Test results with the OTTA (Reference 1) will be of particular value for evaluating multilayer insulation effectiveness in making performance predictions for the HTTA. Thermal performance predictions for the installed insulation system will be included in the contract final report.

For storage of liquid hydrogen over extended periods of time, fluid loss can be reduced by allowing some of the heat leak to be absorbed in the stored liquid, thus producing a rise in storage pressure. Further investigations would be required to determine the feasibility of this type of operation.

A boiler shield is presently more reliable than any other device for preventing liquid from escaping a cryogenic storage sys tem during constant-pressure, zero-g storage. The only other type of device which presently appears feasible is a retention screen device. Current development work indicates, however, that this type of device would weigh as much or more than a boiler shield.

8.0 REFERENCES

(1) Contract NAS9-10348, Propulsion Cryogenic Tankage for Extended Mission Capabilities - Oxygen Thermal Test Article (OTTA), Beech Aircraft Corporation, Boulder Division, final report to be published.

(2) NASA-CR 72605, Thermal Performance of Multilayer Insulation - Interim Report, Lockheed Missiles & Space Company, April 1971.

(3) Leonhard, K. E. and Hyde, E. H., "Flightworthy High Performance Insulation Development", Cryogenic Technology, January 1971.

(4) Contract NAS9-11160, Alternate Space Shuttle Concepts Study - Orbiter Definition, Grumman-Boeing, July 1971.

(5) Contract NAS9-11330, Shuttle Cryogenic Supply System Optimization Study - Master Integrated Systems Task Report, Lockheed Missiles & Space Company.

(6) Contract NAS9-10583, External Insulations - Final Report, Colspan Environmental Systems, Inc., May 1971.

(7) Contract NAS9-150, Apollo Cryogenic Storage Subsystem, Beech Aircraft Corporation, Boulder Division.

(8) Contract NAS9-1100, Lunar Module Supercritical Helium Conditioning Unit, Beech Aircraft Corporation, Boulder Division.

(9) Contract NAS9-10480, Passive Retention/Expulsion Methods for Subcritical Storage of Cryogens - Summary Report, Martin Marietta, Denver Division, July 1971.

DISTRIBUTION LIST:

External Distribution

NASA Manned Spacecraft Center

EP5/W. E. Rice
W. R. Dusenbury
R. K. Allgeier
R. R. Rice
J. C. Smithson
EP2/H. C. Kavanaugh, Jr.

NASA Headquarters - Washington, DC 20546

George C. Marshall Space Flight Center
NASA Aeronautics and Space Administration
Marshall Space Flight Center, AL 35812

E. H. Hyde, S&E-ASTN-PF

John F. Kennedy Space Center
National Aeronautics and Space Administration
Kennedy Space Center, FL 32899

Frank S. Howard, DD-MDD-4

Lewis Research Center
National Aeronautics and Space Administration
21000 Brookpark Road
Cleveland, OH 44135

D. Nored, 500-209

Grumman Aerospace Corporation
Houston, TX 77058

Richard Fox

TRW Systems
One Space Park Drive
Houston, TX 77058

Dennis Vernon, H4/1102

Lockheed Missiles & Space Company
Box 504
Sunnyvale, CA 94088

L. L. Morgan
Bldg. 562, Dept. 66-01

McDonnell-Douglas Corporation
6501 Bolsa Avenue
Huntington Beach, CA 92674

D. Schweikle, Dept. 253
Group BSSO, Mail Code 14

General Dynamics/Convair
Box 1128
San Diego, CA 92112

A. Schuler
Mail Zone 547-30

R. E. Tatro
Mail Zone 584-00

Martin-Marietta Corporation
Box 179
Denver, CO 80201

J. W. McCown